
Universidad Carlos III de Madrid

Escuela Politécnica Superior

Electrical Engineering Department

Bachelor Thesis

Bachelor's Degree in Industrial Technologies Engineering

# Inductive Energy Capture

*Javier Molina Sanz*

supervised by

Dr. Guillermo Robles Muñoz

June, 2016

*Me gustaría dedicar estas líneas a aquellas personas*
*que me han ayudado a llegar hasta aquí,*
*no sólo en los estudios, sino también como persona.*
*Agradecer a Guillermo, mi tutor de este proyecto,*
*por su incansable e incondicional afán por hacerme aprender.*
*A mi familia, mi novia Bea y mis amigos por su apoyo en todo*
*momento y compañeros que han demostrado ser mucho más que eso*
*como Jesús, Sergio o Álvaro.*

*"Es necesario dudar de todo y tanto como sea posible al menos una vez en la vida"*
*René Descartes*

# Author's declaration

I declare that the work in this dissertation was carried out in accordance with the requirements of the University's Regulations and Code of Practice for Research Degree Programmes and that it has not been submitted for any other academic award. Except where indicated by specific reference in the text, the work is the candidate's own work. Work done in collaboration with, or with the assistance of, others, is indicated as such. Any views expressed in the dissertation are those of the author.

SIGNED:
DATE: 22$^{nd}$ June 2016

# Abstract

Several manners of extracting energy have become popular in the last years. In particular, energy from magnetic field captured by inductive principles is one of the most important methods regarding energy harvesting. Obtaining energy from high-power low-frequency signals is currently possible, but the aim of this report goes further.

Partial discharge phenomena are revealed outside the insulation as high-frequency pulsing signals produced under high-voltage situations that contributes to the deterioration of the electrical machinery, causing even their failure. It is very important to localize this phenomenon in order to avoid possible futures breakdowns. This project demonstrates how to extract energy from high frequency inductive phenomena. Particularly, the feasibility to harvest energy from partial discharge occurrence is satisfactorily studied. Several energy levels are accumulated in a capacitor depending on the topology implemented.

Energy from partial discharges pulses has not been accumulated to date. This report discuss a relation between the voltage across a capacitor and partial discharge events leading to a possible detection system.

# Resumen

Varias formas de obtener energía han tomado fuerza en los últimos años. En particular, la energía obtenida a partir del campo magnético por principios inductivos es uno de los métodos mas extendidos de energy harvesting. Obtener energía de señales de alta potencia y baja frecuencia es posible, pero el objetivo de este proyecto va mas allá.

Las descargas parciales se manifiestan como señales pulsantes de alta frecuencia producidas en situaciones de alta tensión aplicada que contribuyen al deterioro de la maquinaria eléctrica pudiendo causar incluso la rotura. Es muy importante localizar este fenómeno para evitar fallos futuros. Este proyecto demuestra como extraer energía a partir de fenómenos inductivos. Concretamente, se estudia la posibilidad de obtener energía a partir del suceso de descargas parciales, llegando a un resultado satisfactorio. Varios niveles de energía se acumulan en un condensador dependiendo de la topología implementada.

Hasta ahora no se ha acumulado energía a partir de las señales de descargas parciales. Este trabajo permite establecer una relación entre la tensión en un condensador y la actividad de descargas parciales permitiendo llevar a cabo un sistema de detección.

# Contents

# List of Figures

# List of Tables

# Abbreviations

| | |
|---|---|
| **AC** | Alternating Current |
| **ASCII** | American Standard Code for Information Interchange |
| **CAD** | Computer Aided Design |
| **DC** | Direct Current |
| **HF** | High Frequency |
| **HFCT** | High Frequency Current Transformer |
| **HV** | High Voltage |
| **IEC** | International Electrotechnical Comission |
| **PCB** | Printed Circuit Board |
| **PD** | Partial Discharge |
| **RF** | Radio Frequency |
| **RFCT** | Radio Frequency Current Transducer |
| **SMA** | SubMiniature version A |
| **UHF** | Ultra High Frequency |
| **VHF** | Very High Frequency |

# Chapter 1

# Introduction

## 1.1. State of art

Energy is everywhere in the environment among us, it is the engine that powers the world. Humankind has managed since a long time ago, to get energy from different sources in order to thrive.

The increasing energy problems and society concerning about them resulted in the birth of energy harvesting. As its own name suggests, it is the process by which energy is obtained from different sources and stored for different purposes. It is a really booming concept that is becoming important due to current energy supply deficit.

Paying attention to the ancient society strongly dependent on mechanical energy, and after the formidable progress of technology, several new ways of extracting energy have arisen. Nevertheless, the unreasonable consumption of energy extracted from fossil fuels is threatening to change life as we know it.

The first observation of energy harvesting was in form of current from natural source in 1826. Thomas Johann Seebeck found that a current would flow in a closed circuit made of two dissimilar metals when they are maintained at different temperatures [1][2].

In [3] a specially designed DC-DC converter and a thermoelectric generator module to broadcast a short-range wireless signal was combined. The DC-DC converter was unique in that is used a switched-capacitor design to handle power supplied by the thermoelectric generator of either polarity to produce an always positive power output. The device is shown to operate from either the heat source of a

warm hand or the heat sink provided by a vessel of cold water.

A novel approach to thermal harvesting using a small greenhouse device to capture thermal energy from solar radiation is proposed in [4]. The greenhouse was used in conjunction with a solar concentrator and a black body heat sink to harvest energy to recharge small nickel metal hydride batteries. The device was capable of recharging an 80 mAh and a 300 mAh nickel metal hydride battery in 4 and 18 minutes, respectively.

Energy harvesting is undoubtedly a noteworthy method for a broad range of self-powered systems. One of the most remarkable examples is the well-known solar energy which provides the highest power density than any other energy harvesting source. While solar harvesting has the higher power density of all harvesting techniques, it is strongly dependent on the intensity and duration of the energy source available. A device called "Heliomote" was examined and designed to perform specific energy storage from two solar cells in [5]. In general, solar panels are used for numerous applications [6].

However, different sorts of energy harvesting sources have recently emerged, energy from the environment is scavenged through the radio frequency. Nokia launched a prototype that was able to harvest energy from the antennas or TV in order to charge slowly its own battery [7]. Aditionally, RF energy can be also used for supplying wireless sensors as in [8].

Another interesting manner to collect energy is taking profit of piezoelectric sensors. Piezoelectric and electrostatic generators were used to convert pressure variations to energy because they provide a high power density. In this way, energy can be extracted from a person running or walking by integrating an electronic system in a footwear as discussed in [9].

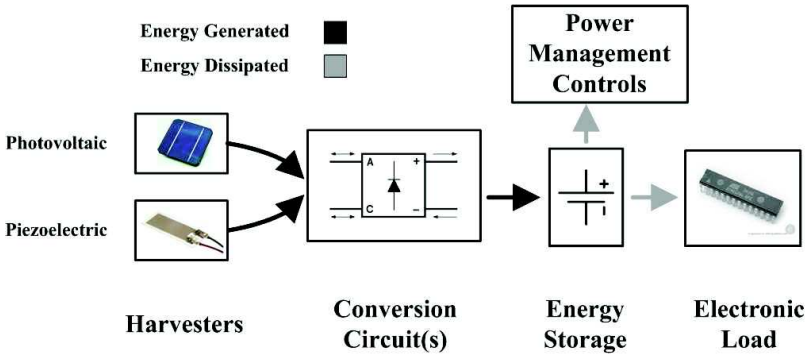


Figure 1: Typical energy harvesting system

Inductive methods for energy harvesting produce a magnetic field from a current and a later voltage is induced. This principle is used for many applications, for example, an energy harvesting system is implemented to convert an store low voltage sinusoidal power induced from magnetic power generators for supplying low power applications [10]. Another example could be a supercapacitor charged by implementing an energy harvesting system taking profit of an aircraft power line with a current of variable amplitude [11]. Power donuts are devices which allow to offer remote monitoring of overhead electrical power lines, conductor temperature, current, voltage are some of the possible measurements offered by this devices [12].

A typical energy harvesting system is composed of several stages: it is necessary a transducer in order to turn a physical phenomena into an electrical magnitude, signal processing as AC/DC signal conversion, an element where the energy is stored and a voltage regulator if needed. This steps are aimed to supply a load in a suitable way to accomplish the energy harvesting goal.

In this work the explanation to obtain energy from inductive phenomena, focusing on partial discharges is discussed. This study is something new, not carried out before.

## 1.2. Motivation

Electrical industrial equipment is nowadays worldwide extended because of its great duty performance, so it is present in most of industries. It is known that electrical machinery life-cycle depends strongly on its insulation status that is hard affected by partial discharge activity since it contributes to its deterioration.

Partial discharges are produced in the insulation of this sort of machinery. The importance of its measuring resides in that, it reveals symptoms of insulation degradation and it permits to estimate the equipment remaining life. Partial discharge can be detected following various techniques.

Finding a manner to take profit of partial discharges, to avoid the progress of insulation deterioration is the objective. A contribution to the energy harvesting concept using partial discharge signals is the main motivation of the present thesis.

# Chapter 2

# Partial discharges

## 2.1. Introduction

According to [13]: "A partial discharge is a localized electrical discharge that only partially bridges the insulation between conductors and which can or cannot occur adjacent to a conductor". They are a direct consequence of a concentration of high voltage stress.

Generally, PD signals appears in certain conditions such a presence of joints, air pockets, gas-filled voids where the air or gas dielectric constant is really small and, as a result, when a voltage is applied to the insulation, the electric field becomes very high. Therefore, PDs are produced under medium heterogeneity constant and strength value. It occurs in insulation systems such as for instance power cables and power transformers.

An intense electrical field causes an ionization in the medium allowing current to flow in an attempt to neutralize the charge separation, which prompts the electrical breakdown and it may lead to failure of the machinery. PD measurement consist on measuring this spark.

Since the electrical field strength within the void depends on the applied voltage and it is an alternating current, PDs take place not only in the positive half but also in the negative one. In Figure 2 it is shown a void inside an insulation, and as aforementioned, the electrical field within the void is high and an electrical breakdown will be produced.

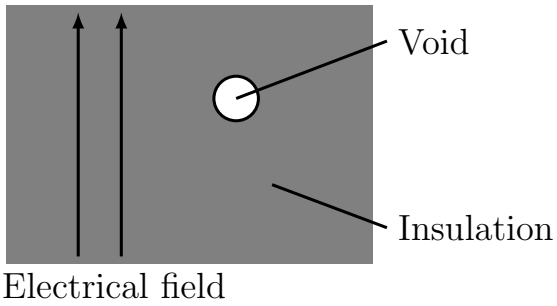


Figure 2: Void inside an insulation

To understand the complex mechanism of PD an equivalent circuit model known as the **three capacitance model** is introduced in Figure 3. It consist of three capacitors and a discharge gap [14]. The capacitor $C_g$ represents the capacitance of the void where partial discharges occur, and capacitors $C_a$ and $C_b$ represent the capacitance of the insulation in parallel and in series with the void, respectively. The discharge gap $G$ is an element such that when the voltage across the gap reaches the inception voltage, $V_i^+$, a discharge occurs and the voltage is reset to the residual voltage, $V_r^+$, by the compensation caused by the discharge.

Discharges also occur in the opposite direction: when the voltage across the gap reaches $V_i^-$ it is reset to $V_r^-$ by a discharge in the opposite direction.

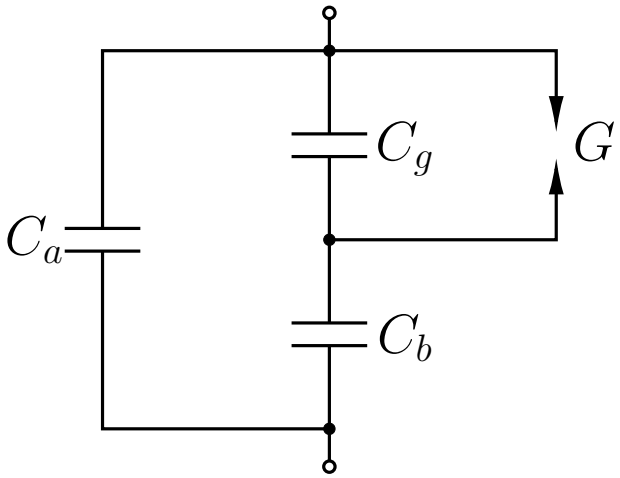


Figure 3: Three-capacitors circuit model

A time evolution is implemented in Figure 4. On one hand, $u(t)$ is the voltage across the gap where partial discharges are likely to occur. On the other hand, $v(t)$ is the applied alternating voltage where is expected not to occur any partial discharge.

As regards, real phenomena $V_i^{\pm}$ and $V_r^{\pm}$ cannot be considered constant since real partial discharges do not necessarily occur and terminate at the set inception and residual voltages. This process is repeated several times creating, on this way, a fluctuating current in both half. So the more discharges are produced, the current flowing through the defect becomes smaller. This current can be used to determine the integrity of electrical equipment and to carry out a predictive diagnostic to estimate the need of maintenance.

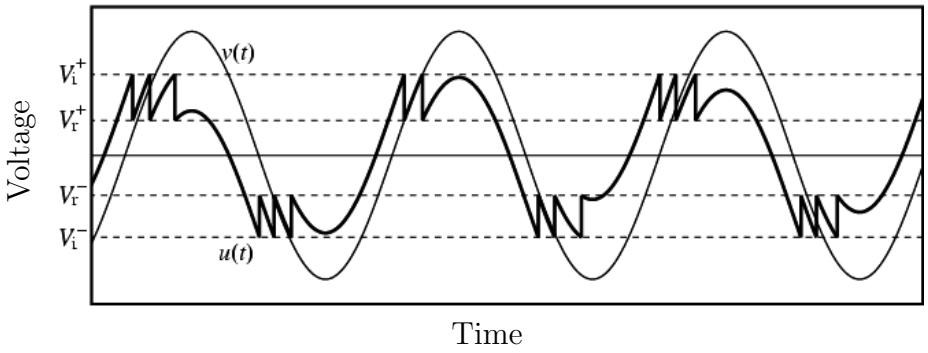


Figure 4: Time evolution [14]

As it is exposed in the previous paragraph, a PD is presented as an extremely brief electrical current to flow through the air pocket whose duration is between a few nanoseconds and microseconds. Partial discharges are presented as very high frequency pulses that have been superimposed to the high voltages. In Figure 5 it is shown an elliptical representation of the voltage applied with PDs occurring.

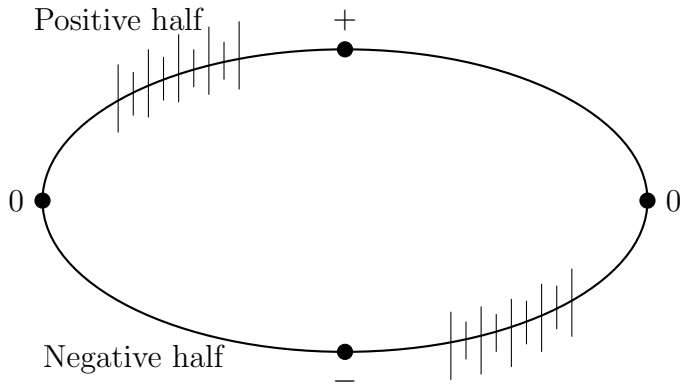


Figure 5: Partial discharge in a period

Regarding its detection, it is fairly difficult to carry out. It can be divided in two main groups, conventional and non conventional methods.

## 2.2. Conventional detection: IEC 60270

DP measuring circuits are detailed in IEC 60270 [15], not only for alternating current but for direct current with a frequency up to 400 Hz.

Table 1 shows all the parameters involved in both circuits, i.e. circuits related to direct and indirect methods.

| | |
|---|---|
| $U$ | High voltage source |
| $C_a$ | Test object |
| $C_k$ | Coupling capacitor |
| Z | Filter |
| $Z_{mi}$ | Measuring system impedance |
| CD | Coupling device |
| MI | Measuring instrument |
| CC | Coupling capacitor |

Table 1: Parameters involved in PD measuring

### 2.2.1. Direct method

As it is shown in Figure 6 the measuring impedance is series with the test object. It is not very common cause this circuit does not pay attention to the safety of the components and a short-circuit can occur.

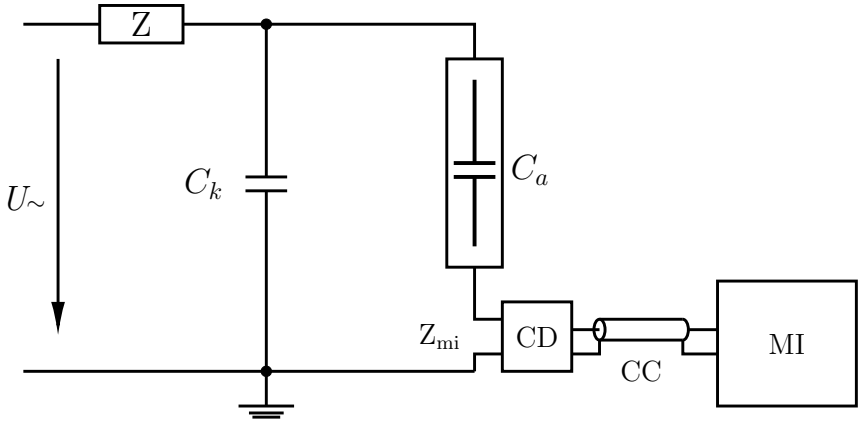


Figure 6: Direct circuit

### 2.2.2. Indirect method

Indirect circuit is exposed and explained in Figure 7. The measuring impedance is series with the coupling capacitor. This circuit is the most common because since the measuring impedance is not series with the test object, damages in measuring instrument are avoided so security at the laboratory is increased.

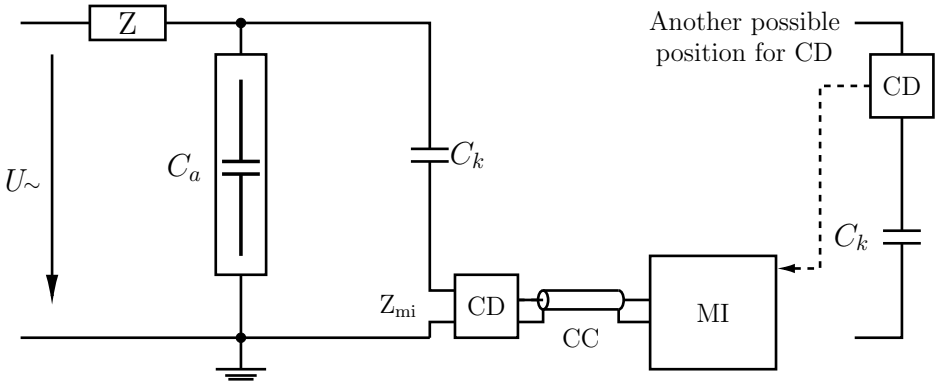


Figure 7: Indirect circuit

Several parameters must be explained to understand the behavior of the circuits:

- Coupling device. A HFCT is used as coupling device, it is also called RFCT and it consist of an induction coil with a ferromagnetic core used for measuring transient signals as PD [16]. For this sort of application, this sensors are exposed as a system, whose input is the PD pulses current and the output is the induced voltage measuring over the input impedance (50 Ω).

  The transfer function of this kind of sensors can be expressed by the Faraday's law.

$$e = -n \cdot \frac{d\phi}{dt} = -n \cdot A \cdot \frac{dB}{dt} = -\mu_s \cdot n \cdot A \cdot \frac{dH}{dt} \tag{1}$$

  Taking into consideration that $\phi$ is the magnetic flux flowing trough the coil with a number of turns $n$ in an area defined as $A$.

  Since a ferromagnetic core is present, (1) can be rewritten as follows.

$$e = -\mu_0 \cdot \mu_r \cdot n \cdot A \cdot \frac{dH}{dt} \tag{2}$$

The voltage in the secondary is clearly proportional to the current in the primary, so let it be $M$ the mutual inductance between the secondary and the earth conductor.

$$e = M \cdot \frac{di}{dt} \tag{3}$$

So the equivalent model of a HFCT sensor can be observed in (8).

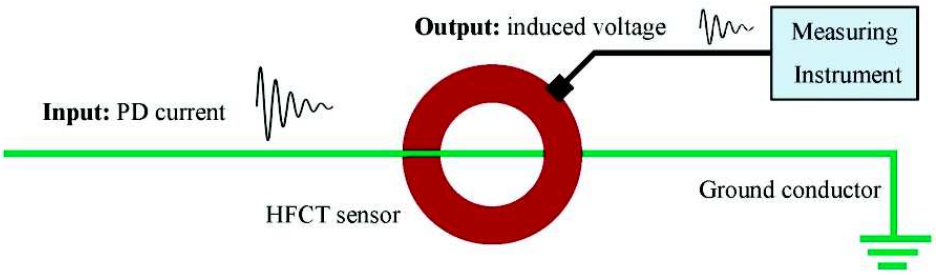


Figure 8: Equivalent model of a HFCT sensor [16]

- High Voltage source. In this case, a transformer is used as a high voltage source. Once the PD signal is produced, a way to ground must be found. Since the signal is in the range of HF, the impedance of the coil is:

$$Z_l = j \cdot w \cdot L \tag{4}$$

  It is easy to check that the impedance of the coil of the transformer will be high as exposed in (4) since PD pulses are high frequency, the transformer impedance prevents high frequency signals, such as partial discharges,to flow into the coil and they have to find another path to ground.

- Coupling capacitor. According to the aforementioned, the coupling capacitor allows the current pulse to flow through it. It is remarkable that this capacitor must present a low PD activity because it could affect the measuring of the test object.

- Test object. It can be modeled as a capacitor because a voltage between it and ground arises. It represents any insulating system.

- Filter. Is an impedance suitable for lowering the electromagnetic noise of the high voltage source.

- Measuring instrument. Different devices are required depending on several parameters as for example, the frequency of the signal, that implies different bandwidths.

In the procedure to analyze PD signals are involved every instrument defined above. The circuit is composed of a capacitive divider, a high voltage capacitor is in series with a measuring impedance, represented in Figure 9. The voltage supplied by the transformer is raised until PD activity is noticeable, then PD signals are conducted through the capacitive branch which offers a low impedance way.

It is important to remark that the pulse is not registered itself, but its occurrence, this is enough to extract quite information about the partial discharge, as for instance the signal size or duration [17].

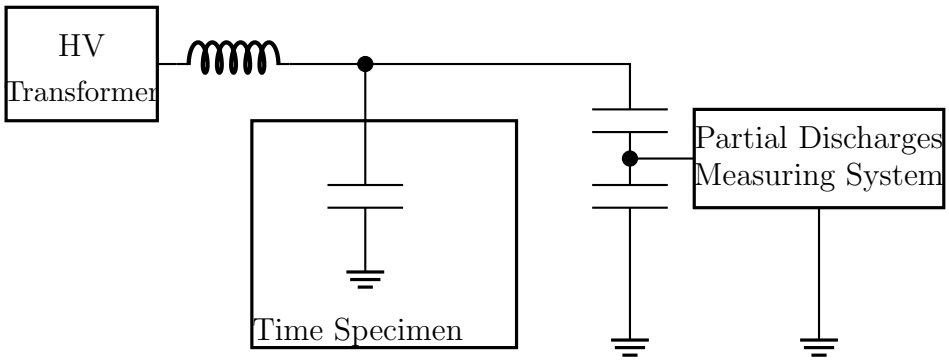


Figure 9: PD measuring circuit [17]

## 2.3. Non conventional detection: IEC 62478

Apart from the conventional method, a new Standard IEC 62478 which covers acoustic and electromagnetic PD detection methods is under preparation, nevertheless an introduction to both methodologies is exposed. This procedures offer some advantages over conventional detection, since an electrical contact is not required which implies a safer situation.

### 2.3.1. Acoustic methods

The acoustic method detects and locates the position of PD by analyzing the amplitude attenuation or phase delay of the acoustic waves propagating from the PD.

For instance, in transformers this waves are caused by the mechanical energy explosion due to the vaporization of the material inside the transformer tank creating pressure waves and, regarding the location, it can be estimated by measuring the time of arrival of the wave [18][19].

Acoustic methods are based on using ultrasonic sensors to detect PDs signals, acoustic transducers such as microphones or piezoelectric sensors are used for this purpose. There are certain situations in which several advantages over others procedures are present. Regarding this case, the acoustic method is immune to electromagnetic noise, which must be taken into consideration in electrical methods since it reduces the sensibility and accuracy of the measurement [20].

### 2.3.2. Electromagnetic methods

Electromagnetic methods consist of a measuring procedure based on radio frequency. Partial discharge pulse signals emit electromagnetic waves suitable for being detected through devices such as antennas. Depending on the frequency range of this waves, a differentiation is necessary between HF, VHF and UHF.

- HF. It includes a range of frequency from 3 MHz to 30 MHz.
- VHF. The frequency range is from 30 MHz to 300 MHz.
- UHF. Suitable for frequencies between 300 MHz and 3 GHz. UHF sensors present several advantages in term of PD measurement which can be summed up in:
  - High immunity to noise and interferences since the frequency spectrum of that signals is really small, even negligible in certain conditions.
  - Great sensitivity inside electrical equipment such as transformer.
  - Accurate PD location thanks to the selectivity in the distance demanded in this method.

  After measuring using UHF sensor, an amplifier is recommended in the output, in that, if low levels signal are evaluated, a later sensibility is required and it is provided by the amplifier.

  Antennas are suitable for detecting this electromagnetic waves but sometimes there are interferences due to the electromagnetic noise present, produced by the radio or Wi-Fi emission so it is important to analyse this fact in order to not to make mistakes with the measurement.

Sometimes it is common to convert the signals from UHF to HF because processing UHF PD signals requires oscilloscopes with a bandwidth over 1 GHz and a 5 GS/s sampling rate, i.e. a expensive device.

Once the methods to capture partial discharge signals are exposed, some of these techniques are going to be carried out to extract energy from partial discharge signals. A focus on the energy obtained from PD signals measured by an inductive sensor (HFCT) is fundamental but the concepts of energy and power must be previously introduced.

# Chapter 3

# Energy and Power

At first, it is necessary to calculate the energy of the signal in order to estimate the power extracted from the partial discharge, so as it is explained below it is mandatory to compute the area of the signal.

The instantaneous power can be calculated as follows [21].

$$p(t) = \frac{1}{R} v(t)^2 \, dt \tag{5}$$

So if we set to 1 Ohm the value of the resistor to simplify (5) can be rewritten as:

$$p(t) = v(t)^2 \, dt \tag{6}$$

So, once the power is calculated, the energy can be obtained following (7).

$$w(t) = \int_0^t p(t) \, dt = \int_0^t v(t)^2 \, dt \tag{7}$$

Since the signal is alternating between positive and negative values, as it is shown in Figure 10, each point of voltage is squared because otherwise positive values would be cancelled with negative ones. Taking into account the sampling frequency, and consequently the sampling period, that is, the time difference between two consecutive points, the power is calculated as the sum of each area divided by the time necessary to get this energy.

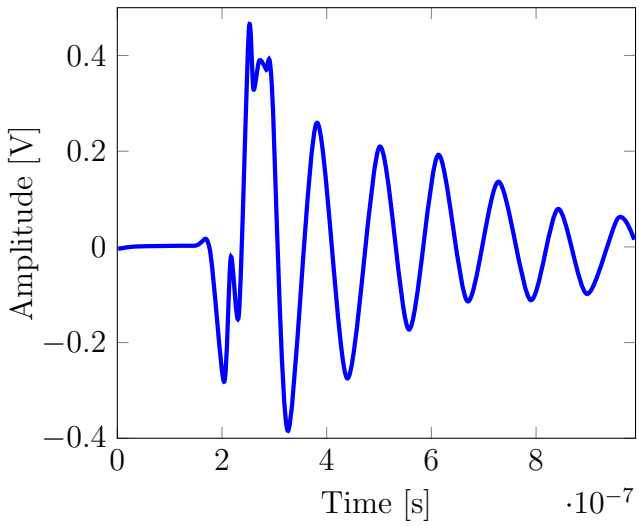


Figure 10: Sample waveform of an electric signal

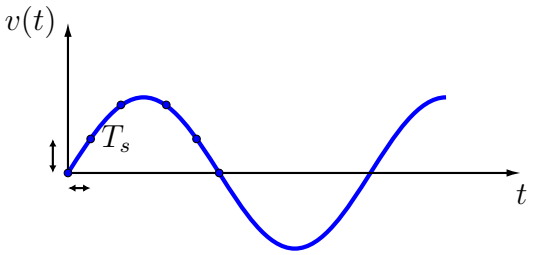


Figure 11: Signal sample time

So, let it be $P$ the average power extracted from the partial discharge signal, $N_p$ the number of points taken and $T$ the time necessary to obtain the signal. Thus,

$$P = \frac{dW}{dt} = \frac{\Delta W}{\Delta t} \tag{8}$$

$$W = \sum_{i=1}^{N_p} V^2 \cdot T_s \tag{9}$$

$$P = \frac{\sum_{i=1}^{N_p} V^2 \cdot T_s}{T} \tag{10}$$

## 3.1. Computation of energy and power

Once the previous concepts are introduced, it is necessary to compute the energy and consequently, the power in order to analyse whether energy could be extracted. A real case is going to be carried out to at the laboratory because it is fundamental to determine whether the energy is high enough to be stored. It is important to remark that the energy from PD signal is going to be obtained from inductive method because the energy emitted in radio frequency is really small.

For this purpose, the conventional method with the indirect circuit is the choice to carry out the measuring. The circuit composed at the laboratory is shown in Figure 12.

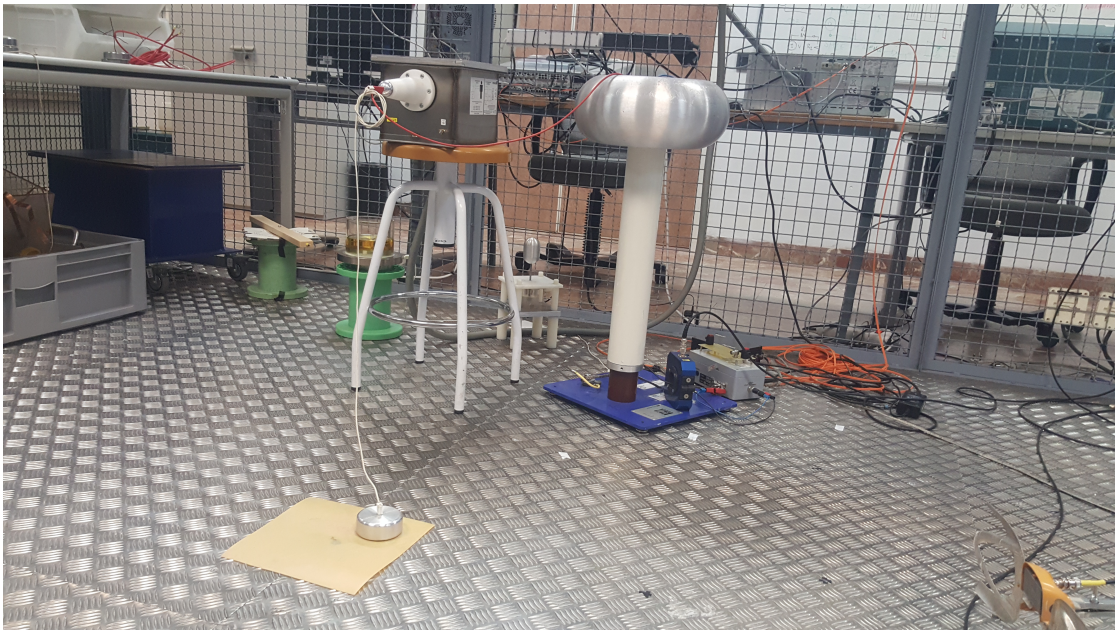

Figure 12: Partial discharges detection circuit

The device employed to visualize the measurement is a Tektronix DPO7254 oscilloscope. The sampling frequency was set to 5 GS/s in signals from DP1 to DP5 and 1 GS/s in signal DP6 and the event duration was fixed to 1 $\mu$s.

The number of samples of a signal is the quantity of points which conform the signal. It is the inverse of the sampling frequency ($f_s$), that is, the average number of samples obtained in one second.

Table 2 collects all the data obtained in the laboratory.

| Name | Number of Signals | Time $[s]$ | Voltage $[V]$ | Trigger $[V]$ |
|---|---|---|---|---|
| DP1 | 100 | 26 | 1460 | 1.570 |
| DP2 | 100 | 154 | 1460 | 1.570 |
| DP3 | 100 | 17 | 1460 | 0.500 |
| DP4 | 100 | 10 | 2500 | 1.470 |
| DP5 | 100 | 28 | 2500 | 1.470 |
| DP6 | 500 | 7 | 2500 | 0.324 |

Table 2: PD experimental results

- The trigger is the voltage limit value set by the user that thereafter signals are visualised. In other words, it is the threshold voltage necessary to start collecting signals. This value must be high enough to avoid appearing electromagnetic noise, but low enough to not to lose signals that could be interesting to analyse.
- Voltage refers to the level of potential applied to the test object. It is applied through the HV transformer.
- The variable called time, refers to amount of time necessary to obtain the number of signal established. The reason of the different values of this parameters is explained later.

Then, in order to calculate the number of samples present in a signal is necessary to expose the next formula.

$$\text{Event duration} = \frac{N_p}{f_s} \tag{11}$$

So, accordingly:

$$N_p = f_s \cdot \text{Event duration} \tag{12}$$

Thus, the number of samples for DP1 to DP5 matrices is:

$$N_p|_{\text{DP1-DP5}} = 5\frac{GS}{s} \cdot 1\mu s = 5000 \text{ samples} \tag{13}$$

The number of samples for DP6 matrix, will be different, since the sampling frequency was modified.

$$N_p|_{\text{DP6}} = 1000\frac{GS}{s} \cdot 1\mu s = 1000 \text{ samples} \tag{14}$$

The reason why some measurements are repeated is necessary to be explained. PD activity decreases with time, so at the beginning more signals can be captured. It can be noticed that, analyzing the variable called time, for DP1 matrix the number of signals is 100, the same for DP2. The voltage applied to the test object is the same in both cases and the trigger, that is, the threshold voltage, remains constant. On the contrary, the time varies which implies that, for the same number of signals to capture with the same voltage applied and the same trigger, is necessary more time.

The same reasoning can be extrapolated for DP4 and DP5 signals, the second one is after a few seconds when PD activity decreased, but the difference from the previous case is that, in that signals, the voltage has been raised up to 2500 V.

On the other hand, for the analysis of DP3 the trigger was set to 0.5 V with the purpose of detecting more signals because with a higher value for the trigger signals with a voltage lower than this threshold values are lost. It can be seen that, for the same voltage of the source and remaining constant the number of signals captured, the time is shorter than for DP1 and DP2 signals, fact which makes sense since the trigger has been lowered, i.e. more signals are detected and, consequently, the time to get the same number of signals is reduced.

As to DP6, it is remarkable that the number of signals have been set to 500 with a voltage of 2500 V and the trigger is lowered up to 0.324 V. Checking the results, in spite of having multiplied by five the number of signals, the time is strongly reduced, in that, the trigger is low. Once the signals have been saved, exporting them to *Matlab*, to calculate the energy and power, is a must.

Therefore, several decisions can be made. First, as higher the level of voltage applied to the circuit PD activity is more intense and accordingly, the power available would be greater. However, it is very difficult to determine the number of PD signals because this value depends on several parameters; the trigger which allows to measure more signals impinges strongly on the signals detection. For this case, it is better to set a low trigger instead of a higher one because more signals will be received in the oscilloscope. The time also affects to the PD activity because at the beginning more signals are produced, but it tends to become steady when the times goes on.

| Name | Energy [J] | Power [W] |
|---|---|---|
| DP1 | $7.4890 \times 10^{-6}$ | $2.8804 \times 10^{-7}$ |
| DP2 | $6.4617 \times 10^{-6}$ | $4.1959 \times 10^{-8}$ |
| DP3 | $2.5725 \times 10^{-6}$ | $1.5133 \times 10^{-7}$ |
| DP4 | $1.4093 \times 10^{-5}$ | $1.4093 \times 10^{-6}$ |
| DP5 | $1.2334 \times 10^{-5}$ | $4.4048 \times 10^{-7}$ |
| DP6 | $2.3742 \times 10^{-5}$ | $3.3917 \times 10^{-6}$ |

Table 3: Computation of energy and power

In conclusion, it is not possible to determine the number of PD signals and accordingly, the power available. However, it can be stated that the higher the voltage applied, the higher the number of PD signals.

## 3.2. Estimation: Charging a battery

After the estimation of the power extracted, a first intention is to store the energy in a battery. Consequently, it is easy to calculate the time necessary to charge a 0.7 mA·h and 3.2 V battery, that would be enough to supply a micro system as for example a sensor as discussed in [22].

As the signal which provides more energy is DP6 signal (see Table 3) this would be used to charge the battery. Thus, the definition of power is:

$$P = V \cdot I \tag{15}$$

So, the current demanded can be calculated as follows:

$$I = \frac{P}{V} = \frac{3.39\ \mu W}{3.2\ V} = 1.059\ \mu A \tag{16}$$

Taking into consideration that the capacity of the battery is 0.7 mA·h, the time to fully charge the battery is:

$$t = \frac{0.7 \cdot 10^{-3} A \cdot h}{1.059\ A} = 660.4\ h \tag{17}$$

According to the results, it would be a tough task to verify this charging process during this long period of time because the laboratory must be supervised. Besides, it is only a first estimation, several conditions must be analyzed since this is how an ideal situation would be developed following a power balance, but another factors as, for instance, power losses or being able to extract this energy, ought to be considered. To sum up, the idea of charging a battery is rejected because of its time necessary to be charged.

# Chapter 4

# First approach

The results show that the signal which provides more energy and power is signal called DP6 and that is why the next steps will be implemented from that. As the duration of DP6 signal shown in Figure 13 is 1 $\mu$s, it is very difficult to notice the voltage rise across the capacitor because it is a pulsating alternating signal and in addition to this it is a very short signal.

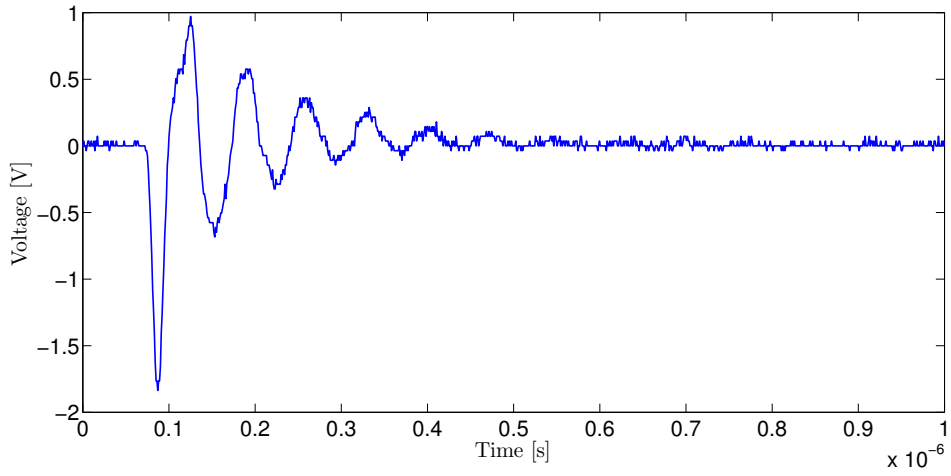


Figure 13: Partial discharge signal

Firstly, the concept of diode and capacitor are introduced. A diode is a two terminal electronic component which conducts primarily in one direction. It allows several functions but in this project one of them is carried out. Diodes can act as a rectifier allowing the current flow in one direction, i.e. turn alternating current into direct current.

(a) Capacitor symbol (b) Diode symbol

Figure 14: Capacitor and diode scheme

A capacitor is a passive device that stores energy in its electric field and returns energy when it is required.

These devices are going to play an important role in this project. On the one hand, the diode is going to be necessary to permit the current flow only in sense to rectify the signal. On the other hand, the capacitor is the first element used for storing energy.

A first approximation is going to be carried out using Simulink in order to estimate the power storage capacity. The objective of this part of the project is storing energy in the capacitor, so a rectification of the signal is going to be carried out. Since a diode is not included in Simulink software, to simulate the behavior of an ideal diode the absolute value of DP6 signal is taken. Figure 15 would be the result obtained after rectifying the signal with an ideal diode.

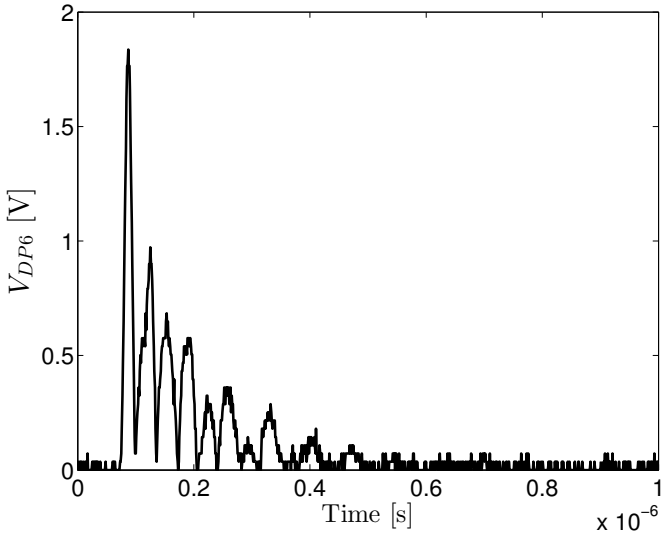


Figure 15: Absolute value of DP6 signal

Once the signal is rectified, a simulation to notice the voltage rise is necessary. As the signal length is really small, to see the evolution of the voltage across the capacitor more signals would be inevitable in order to check the time evolution.

A signal called "desc" is created. It is composed of four DP6 signals concatenated one after the other through *Matlab*. By doing this, a simulation of several PD rectified signals is introduced. The result is exposed in Figure 16.

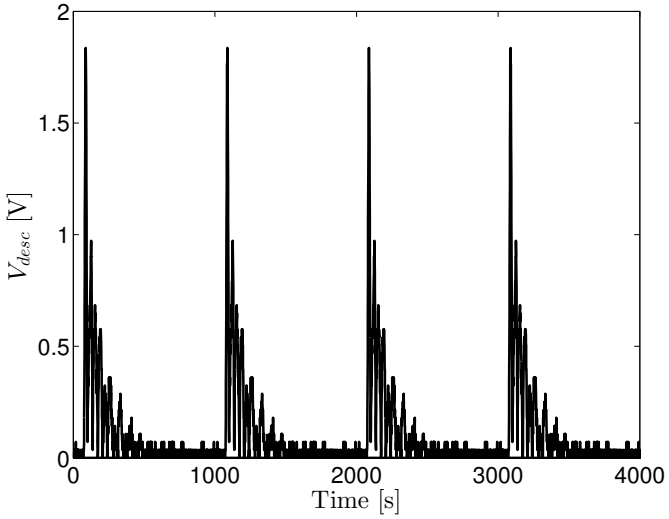


Figure 16: Desc signal

To check the evolution of the circuit, an initial simulation with Simulink is needed. The circuit is composed of a voltage source imported from Simulink, a resistor that simulates the behavior of a diode since it prompts a voltage drop because it is a non ideal component and a capacitor to be charged up. The value of the resistor is set to 6 Ω, which is a typical value for the internal resistance of a diode provided by the datasheet. Different values of capacitance will be evaluated.

As aforementioned, diode is not included in Simulink library and the PD signal must be rectified, i.e. it is required to keep the signal in positive cycles, so as it was explained "desc" is the absolute value of DP6 signal.

A typical RC circuit (Figure 17) is implemented through a transfer function as follows

$$V_c = V_{in} \cdot \frac{1/Cs}{R + 1/Cs} = \frac{V_{in}}{RCs + 1} \tag{18}$$

where $V_{in}$ is "desc" signal imported from Matlab.

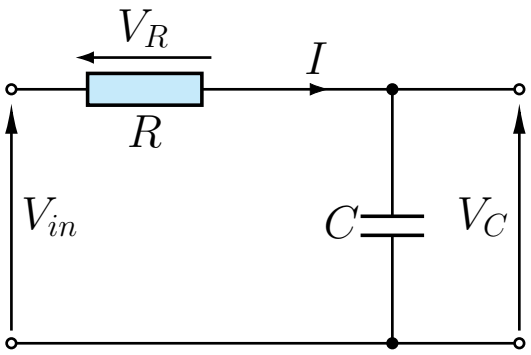


Figure 17: RC circuit

When a capacitor is connected to a DC power, two processes, which are called charging and discharging happen in specific conditions.

To estimate the time necessary to charge and discharge a capacitor, the concept of time constant is introduced, that is, the product of resistance and capacitance. According to this, the smaller the resistance or the capacitance, the faster the charging and discharging processes. But, as a matter of fact, the time necessary to charge and discharge the capacitor is approximately 5 times the time constant as exposed in [23].

$$\tau = R \cdot C \tag{19}$$

Thus, several values of capacitance are evaluated for the simulation, as the equation shows, if the resistance remains constant, a smaller capacitance means a lower time to charge the capacitor but also implies a low discharging time that is not appropriate for capturing energy purposes. The whole diagram is shown in Figure 18.

On the one hand, in order to import the data from Matlab to Simulink the use of a "From Workspace" block is necessary. On the other hand, for importing data from Simulink to Matlab after the simulation of the model, a "To Workspace" block is required.

In Figure 19 is exposed the simulation of the RC circuit implemented through Simulink using a capacitance of $100nF$ is shown. The voltage across the diode raises progressively but in a slow manner. As it was expected, when the "desc" signal reaches its peak value (the same occurs for $V_{cap}$), but since the signal is a pulse one, there is a time interval when the signal is near 0, consequently, the capacitor starts the discharging process until a new signal is received.

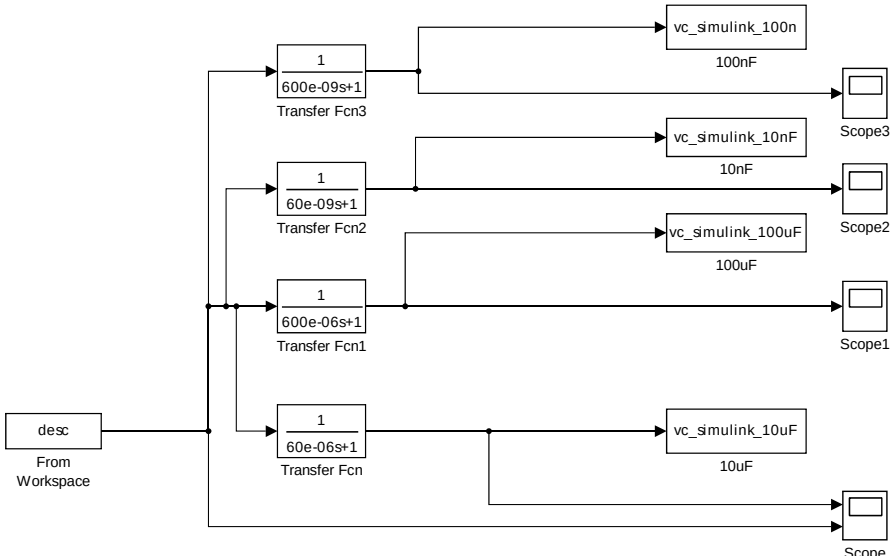


Figure 18: Simulink transfer functions

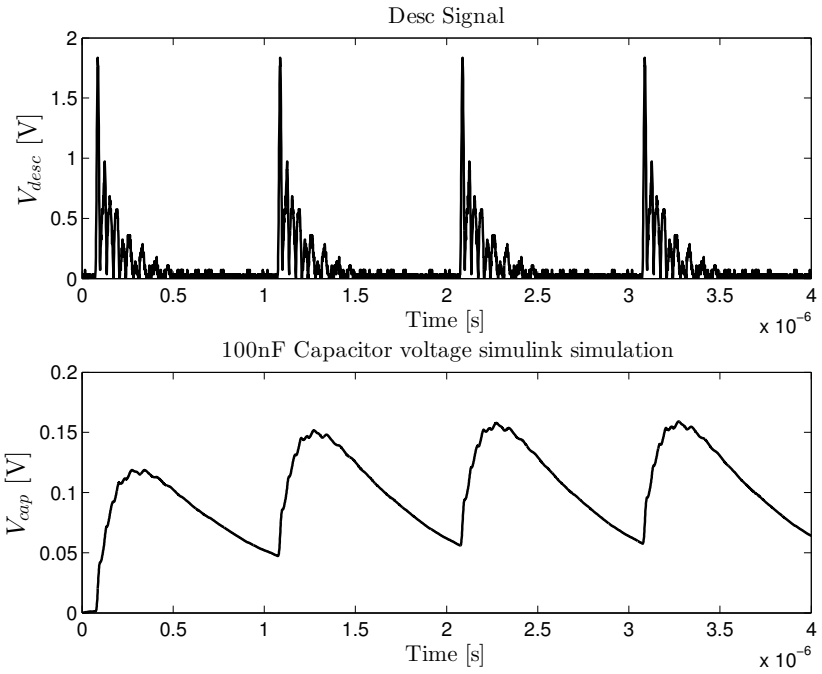


Figure 19: 100 nF Simulink simulation

It is important to remark that, after the first signal, the value of $V_{cap}$ is not 0, so energy is being stored.

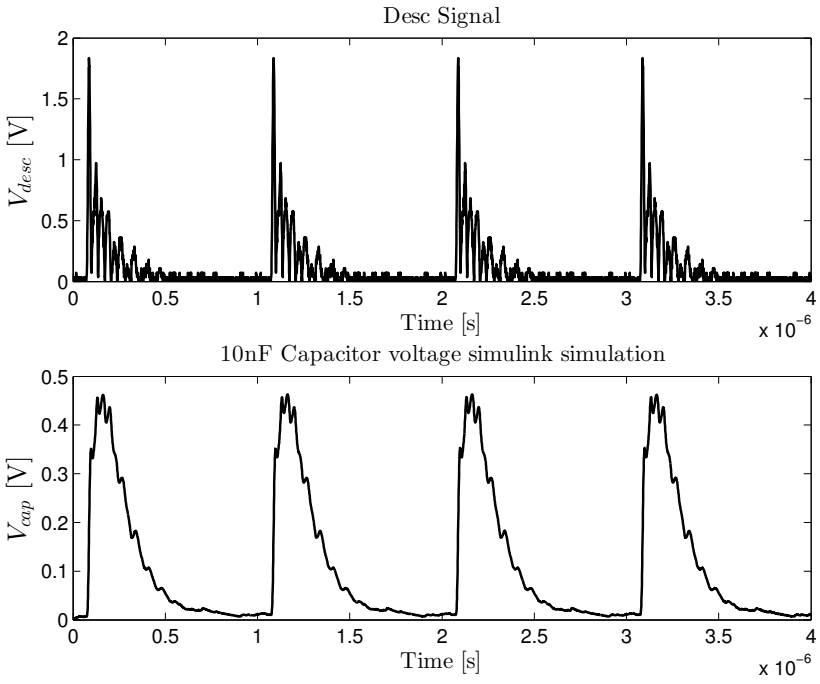


Figure 20: 10 nF Simulink simulation

In Figure 20, the voltage rise reaches its maximum in $0.5V$, higher than the previous simulation. It makes sense because the capacitance is smaller and according to this, the time constant will be smaller too.

On the contrary, this is not only and advantage but also a disadvantage because the discharging process will occur faster. It can be seen that, the time gap when "desc" is approximately 0 is enough to discharge almost completely the capacitor.

In Figure 21 the maximum voltage for the capacitor after the whole signal is 7 mV, pretty far from the previous cases. It is remarkable, that the time constant is high enough to avoid starting the capacitor discharging process.

In Figure 22, the voltage across the capacitor rises very slowly, the maximum value for the voltage is 0.7 mV after the four signals. The prevailing tendency is increasing but much time will be necessary to capture energy.

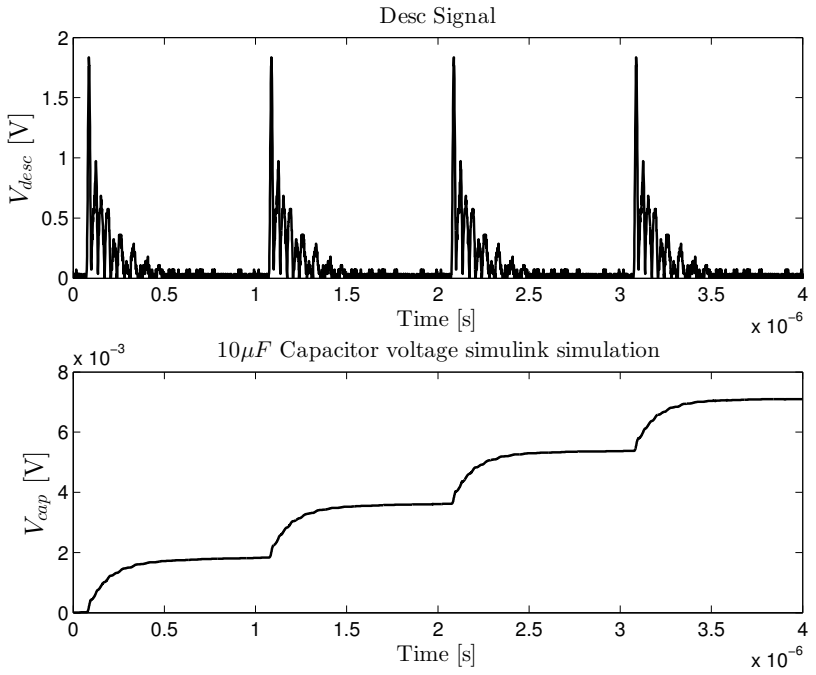


Figure 21: 10 $\mu$F Simulink simulation

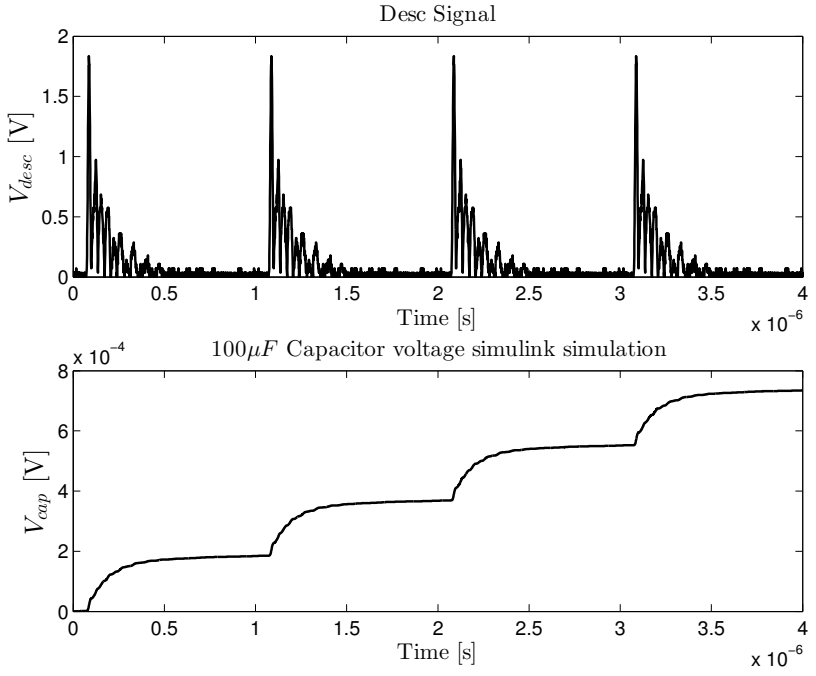


Figure 22: 100 $\mu F$ Simulink simulation

## 4.1. Results

After analyzing the results, a decision can be made. On the one hand, 10 nF capacitor is charged up to the highest value, however, it is discharged very quickly, so the energy storage is not viable. If the results provided from 10 $\mu$F and 100 $\mu$F are analysed the voltage across the capacitor is really small but the discharging process is not started.

100 nF capacitor is the choice for going forward with the simulation, the discharging process can be noticed, but is not fast enough to completely discharge the capacitor, so that energy is stored.

To analyse the decision made, the definition of energy stored in a capacitor is included.

$$E = \frac{1}{2} \cdot \frac{Q^2}{C} \tag{20}$$

Since the capacitance is the ratio of charge on each conductor and the voltage $V$ between them.

$$C = \frac{Q}{V} \tag{21}$$

So if (21) is included in (20) the result is:

$$E = \frac{1}{2} \cdot C \cdot V^2 \tag{22}$$

So, taking into consideration (22) which expresses the quantity of energy that could be stored in a capacitor, checking the capacitor election is a must.

As it is seen, the energy is proportional to the capacitance and the square of the voltage, a calculation of the energy stored in each case can be easily done [24][25].

$$E_{100nF} = \frac{1}{2} \cdot C \cdot V^2 = \frac{1}{2} \cdot 100 \cdot 10^{-9} \cdot 0.06^2 = 1.8 \cdot 10^{-10}\ J$$

$$E_{10nF} = \frac{1}{2} \cdot C \cdot V^2 = \frac{1}{2} \approx 0$$

$$E_{100\mu F} = \frac{1}{2} \cdot C \cdot V^2 = \frac{1}{2} \cdot 100 \cdot 10^{-6} \cdot (7 \cdot 10^{-4})^2 = 2.45 \cdot 10^{-11}\ J$$

$$E_{10\mu F} = \frac{1}{2} \cdot 10 \cdot 10^{-6}\ C \cdot V^2 = \frac{1}{2} \cdot 10 \cdot 10^{-6} \cdot (7 \cdot 10 \cdot 10^{-3})^2 = 2.45 \cdot 10^{-10}\ J$$

Based on the results, it would be logical to go forward with 10 $\mu$F capacitor because it is able to store more energy, but it is important to observe (19) because of its dependence on the capacitance, the time to fully charge the capacitor is 100 times higher with the 10 $\mu$F so the election to go deeper with the simulation is 100 nF.

# Chapter 5

# Deeper simulation

## 5.1. Diode selection

The next step is to determine the diode necessary to do the simulation. Considering that the sample time is very short, a Schottky diode is chosen because this sort of diode provides a very fast switching action and a low forward voltage drop, this is really important, especially for power rectification purposes because power losses would be greater for a higher forward voltage drop and less energy would be accumulated.

Another important reason why this diode is elected is that low power signals are being studied and a low forward voltage diode is needed.

Any electronic device passing current develop a voltage across it. This is called forward voltage of a diode and it arises for two reasons [26].

- There are power losses in the device because of its resistive behavior.
- The turn on voltage of the diode that depends on the semiconductor material the diode is built. This material governs the turn on voltage for the diode. For instance, it is near 0.6 V for silicon and 0.3 V for germanium.

This is a very important parameter to take into account because signals with a voltage below forward voltage could be analysed, so it is mandatory to choose an as low forward voltage diode as possible.

The election is Avago's HSMS286x Schottky detector diode [27] since it is designed for low power input applications at frequencies below 1.5 GHz with a forward voltage of 0.3 V and, accordingly, meets every requirement.

## 5.2. Peak detector

Once the election of the diode has been carried out, a peak detector circuit is performed to accumulate energy in a capacitor.

A peak detector is a series connection of a diode and a capacitor that provides a DC output voltage equal to the peak value of the applied AC signal [28].

The capacitor is charged up to the peak signal of the input. As the diode conducts only positive half cycles, if the input signal falls below peak value, the diode is reverse biased blocking current flow back to the source. According to this, the capacitor retains the peak value even as the input waveform drops to zero.

It is really easy to understand that the provided output signal is not going to be exactly the peak value of the input signal because the diode is a non ideal component. Here resides the importance of a low forward voltage drop diode, since the lower voltage drop, the higher the value of the peak detector output.

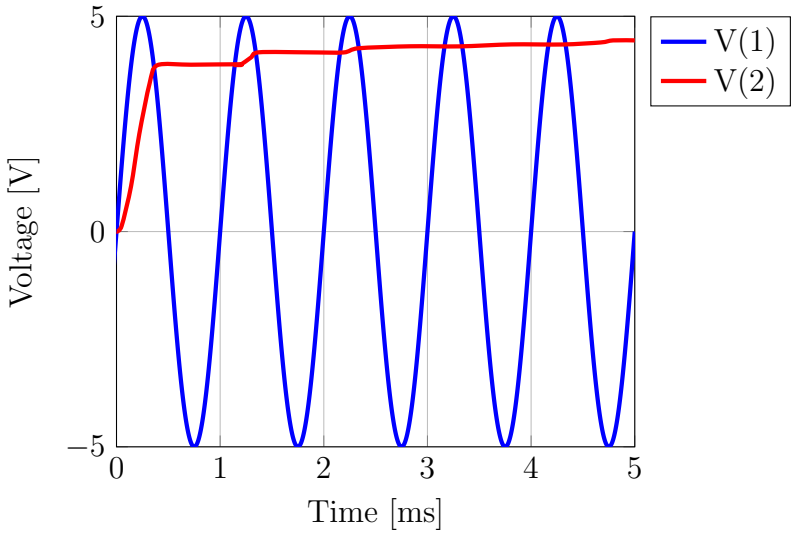


Figure 23: Peak detector sample

It can be shown in Figure 23 that the output voltage is lower than the input, as it has been explained above. The voltage across the diode (the red signal) rises up to certain value depending on the voltage drop of the diode.

The aim is to establish a relation between the voltage across the capacitor and the source voltage.

The current-voltage behavior of a single diode is described by the Richardson equation [29][30].

$$I = I_s \left[ e^{\left(\frac{q \cdot Vd}{n \cdot K \cdot T}\right)} - 1 \right] \tag{23}$$

where $I_s$ is the saturation current, $q$ is the charge of an electron, $V_d$ is the voltage across a diode, $T$ is the temperature in degrees Kelvin and $K$ is Boltzmann constant.

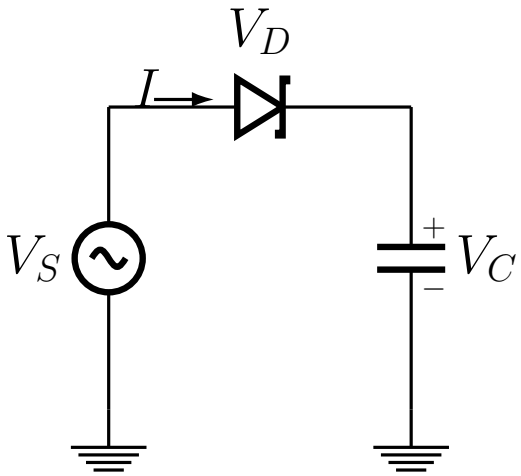


Figure 24: Peak detector circuit

In Figure 24$V_c$ is the voltage across the capacitor and $V_s$ is the voltage of the source.

The voltage equation around the loop shown in Figure 24 is exposed below.

$$V_c = V_s - V_d$$

The current flowing through the diode and the capacitor is the same and the equation can be integrated over a time period, so $V_c$ can be expressed in terms of $V_s$, taking as zero the current of the diode.

$$I_s = \frac{1}{T} \int_0^T \left( e^{\frac{qV_D}{KT}} - 1 \right) dt \tag{24}$$

$$V_C = \frac{K \cdot T}{q} \ln \left[ \upsilon_0 \left( \frac{q \cdot V_S}{K \cdot T} \right) \right] \tag{25}$$

where $\upsilon_0$ is the modified Bessel function of the first type. The value of the $i_d$ is set to zero since the current is very low and it results in the next equation.

If we are interested in low power signals, it is obtained:

$$\upsilon = 1 + \frac{1}{4} + \frac{1}{64}z^2 + ...$$

Letting $z = \frac{qV_s}{KT}$ and taking only the first two terms an approximation can be done.

$$V_c \approx \frac{KT}{q} \ln\left(1 + \frac{q^2V_s^2}{4K^2T^2}\right) \cong \frac{qV_s^2}{4KT} \tag{26}$$

It is called square low operation but a further expansion of this model could be performed as exposed in [29].

So, the equation shows that for a small input signal, the output voltage is proportional to the square of the input signal. Thus, a relation between the voltage across the capacitor and the voltage of the source is established.

If a larger signal is being studied a further approximation can be carried out.

$$V_c = V_s - \frac{KT}{2q} \ln\left(\frac{2\pi qV_s}{KT}\right) \tag{27}$$

In this case, $V_c$ varies strongly as $V_s$ and the detector is said to work in its peak detecting region.

This would be the behavior of an ideal peak detector, but this project is more complex and several conditions must be taken into account. The voltage of the source is not a sine wave, but a pulse signal and PD signals are really fast (nanoseconds) with alternating values, so a simulation to understand how a peak detector works in such situation is recommended.

The circuit will be evaluated for different values of capacitance using Pspice in order to analyze the influence of the capacitance in the capacitor charging regarding the time constant.

## 5.3. Pspice simulation

*Orcad EE Pspice* is a powerful circuit simulator application for simulation and verification of analog and mixed-signals circuits. What makes strong Pspice is

the possibility to simulate real components from electronics manufacturers using a Pspice library provided by them.

A deeper analysis is carried out using *Orcad Capture*. This software lets include an external voltage source imported from a file. According to this, a ".txt" file which contains the time and the voltage in two columns is generated through Matlab.

VPWL_FILE_REPEAT_FOREVER is a Pspice tool which allows to repeat the voltage source imported from an external file during a fixed time set by the user. It is really important for this project in order to simulate several PD signals and analyze the quantity of energy captured in different configurations.

A peak detector will be evaluated for different values of capacitance using Pspice in order to analyze the impingement of the capacitance in the charge of the capacitor.

To start with, every component must be placed in a new project and joined through a wire, but the Pspice model for HSMS286X diode is not available neither Pspice nor on the manufacturer website so it is necessary to create a new model from a default diode model.

Hence, the initial diode parameters must be replaced with the values from the datasheet (Table 4).

| **SPICE Parameters** | | |
|---|---|---|
| **Parameter** | **Units** | **Value** |
| $B_V$ | V | 7.0 |
| $C_{J0}$ | pF | 0.18 |
| $E_G$ | eV | 0.69 |
| $I_{BV}$ | A | $1 \times 10^{-5}$ |
| $I_S$ | A | $5 \times 10^{-8}$ |
| $N$ | - | 1.08 |
| $R_S$ | Ω | 6.0 |
| $P_B$ $(VJ)$ | V | 0.65 |
| $P_T$ $(XTI)$ | - | 2 |
| $M$ | - | 0.5 |

Table 4: HSMS286x diode Spice parameters

Once the new model of the HSMS286x diode is created, the circuit can be implemented. The result is shown in Figure 25.

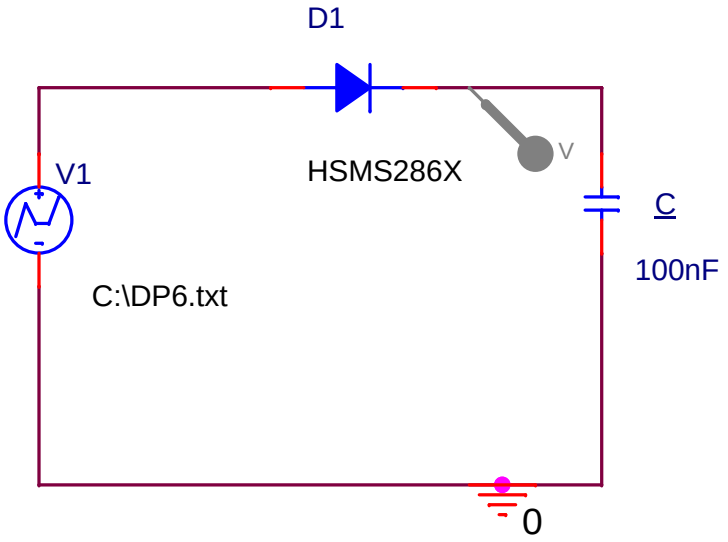


Figure 25: Implementation of the circuit

In this model, $V1$ is an external voltage source imported from Matlab, it is shown in Figure 13. The number of samples of the signal is 1000 as (14) shows but it is repeated during 30 ms one signal after the other. $D1$ is the model created in "Model editor" from Pspice, it is the Schottky diode elected in order to run the simulation.

Several values for the capacitance are evaluated in order to check the behaviour of the peak detector. The simulation time is set to 30 ms in order to observe enough signals to notice the evolution of the voltage across the capacitor.

The number of signals received in 30 ms can be easily calculated taken into consideration that one signal lasts 1 $\mu$s.

$$\text{Number of signals} = \frac{30 \cdot 10^{-3}\, \mu s}{1 \frac{\mu s}{signal}} = 30000$$

In Figure 26 it is shown the evolution of the voltage across the 10 $\mu$F capacitor. A voltage rise, up to 0.55 V is shown. At the beginning, the slope of the voltage is very high but in the end it tends to an horizontal line.

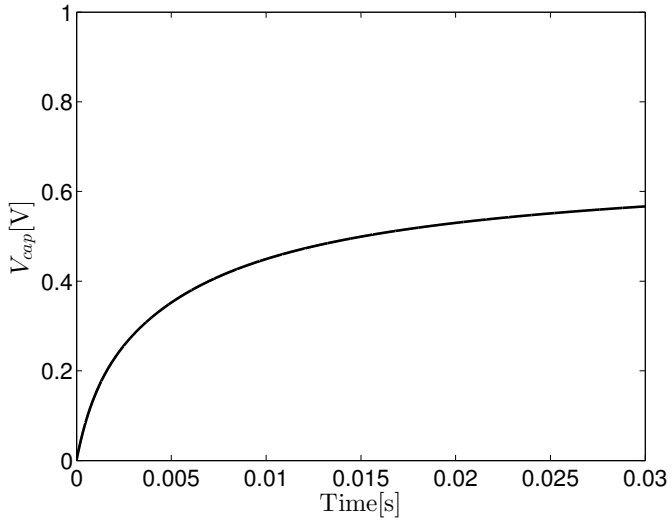


Figure 26: 10 $\mu F$ Pspice Simulation

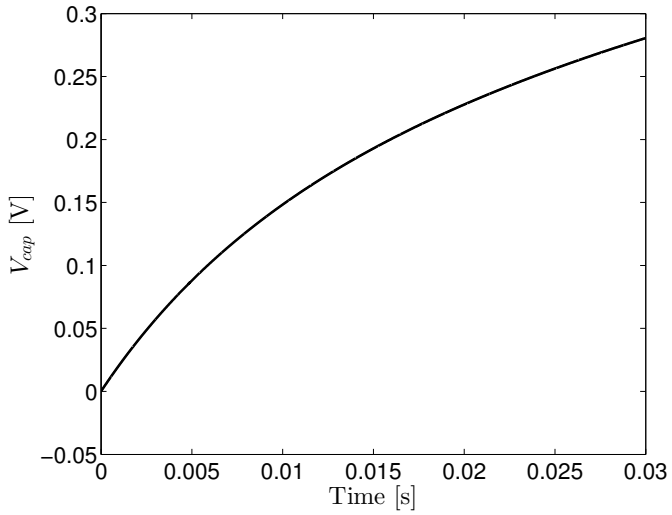


Figure 27: 100 $\mu F$ Pspice Simulation

The voltage across the capacitor of 100 $\mu$F is exposed in Figure 27. The tendency is nearly linear but the voltage rise is up to near 0.3 V, i.e. less than the previous case. It makes sense because the time constant is bigger since the capacitance is 10 times higher.

In contrast with the 10 $\mu$F capacitor, there is no an ultimate horizontal line tendency.

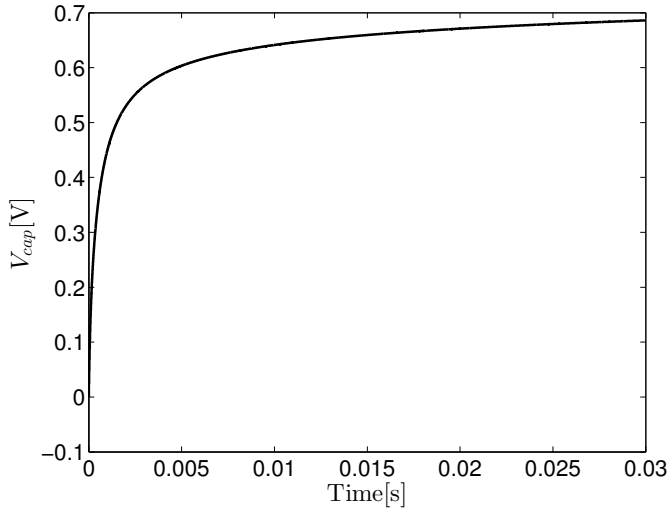


Figure 28: 100 nF Pspice Simulation

It is noticeable that in Figure 28 the voltage across the capacitor tends to 0.7 V, most of the voltage rise happens at the beginning of the signal and after 5 ms approximately the slope is strongly reduced. It tends to became steady when the value of 0.7 V is reached.

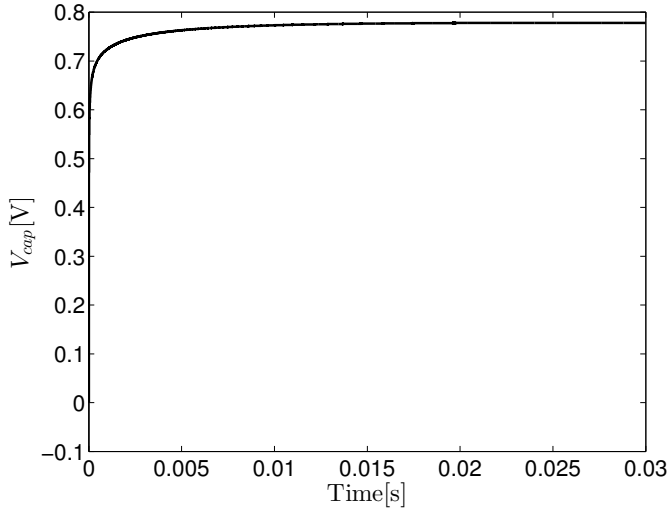


Figure 29: 10 nF Pspice Simulation

As it was expected, the voltage across this capacitor is the highest of the four simulations as it can be seen in Figure 29, this is due to the smaller the capacitance, the shorter the time constant, that is, less time is necessary to fully charge the capacitor if the capacitance is smaller.

As the time is the same for every case, the voltage rise is greater for the lower capacitance capacitor.

## 5.4. Results

After the comparison among the different study cases, several conclusions can be extracted. As lower the capacitance, higher the voltage across the capacitor. It is related to (19), because a lower time constant, implies that the time necessary for charging the capacitor is also smaller.

On the other hand, it seems to have a tendency to became constant near 0.8 V, regardless the capacitance. For 100 $\mu$F and 10 $\mu$F capacitors the simulation time is not long enough to demonstrate that it tends to a constant value but it is likely to happen.

Since the aim of this project is to collect energy, an estimation of the energy stored in the capacitor must be done. Since the highest value for the voltage across the capacitor seems to be 0.8 V because the voltage evolution tends to become steady near this value, the energy stored will be:

$$E = \frac{1}{2} \cdot C \cdot V^2 = \frac{1}{2} \cdot 100 \cdot 10^{-9} \cdot 0.8^2 = 3.20 \cdot 10^{-8}\ J \tag{28}$$

Considering the results, it is a very low power quantity. It depends on the capacitance of the capacitor, that it was set to 100 $\mu$F and the voltage across the capacitor that seems to reach a maximum value which must be taken into account.

As expected, the peak detector does not work ideally since these signals are really fast and short. The peak value for the positive cycles of DP6 signal shown in Figure 30 is approximately 1 V, and the maximum value for the voltage across the capacitor is near 0.8 V. An explanation must be found to determine why the peak detector does not work properly.

The peak value of the signal in the positive half is near 1 V and this value for the negative half is 1.8 V, but the voltage in the capacitor is rectified from the positive half so the reference value is 1 V.

To try to understand the behavior of the peak detector in this situation a simulation of the voltage across a 100 nF capacitor after one signal is exposed in Figure 31.

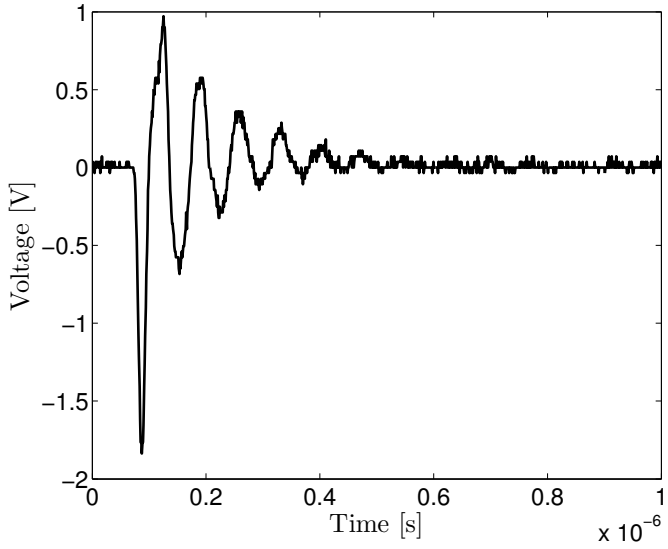


Figure 30: DP6 signal

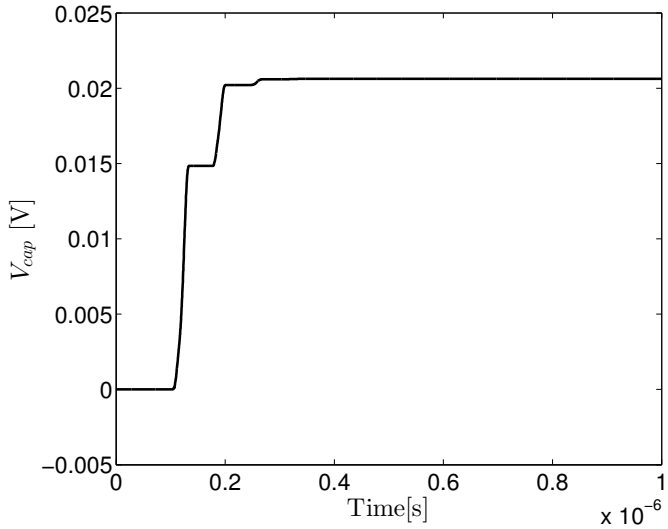


Figure 31: $V_{cap}$ for 100 nF capacitor

If the voltage across the capacitor is analyzed, it is pretty far from the peak value of the input signal since it is very fast and the time constant of the capacitor might be higher. According to this, it would be necessary more time to charge the capacitor.

It is known that is required approximately five times the value of the time constant in order to charge fully the capacitor.

To estimate an approximate value for the time constant of the capacitor it is necessary to obtain the equivalent model exposed of the used diode (Figure 32), this information is provided by the datasheet.

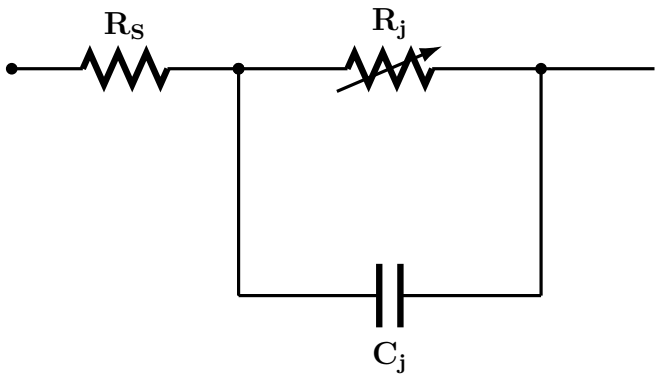


Figure 32: Equivalent model for HSMS286x diode

In the model proposed, $Rs$ is 6 $Omega$ as it is exposed in diode features. In order to do a first approximation, let it consider negligible the value of the rest of the circuit.

$$\tau = R_s \cdot C = 6\Omega \cdot 100 \cdot 10^{-9} F = 600\text{ns} = 0.6\mu s$$

So the time necessary to fully charge the capacitor according to [23] would be approximately:

$$5 \cdot \tau = 5 \cdot 0.6\ \mu s = 3\ \mu s$$

Now a comparison between this time and the rise time for the first peak of DP6 signal must be done.

It can be noticed above in the Figure 30, that the rise time for DP6 signal is approximately 0.15 $\mu$s, that is, the capacitor could not be charged because the time necessary to get the capacitor fully charged is 20 times higher than the PD signal rise time. It is necessary to remark that in spite of having neglected $R_j$ and $C_j$, the result would have been the same since this parameters are of the same order of magnitude and the variation in the time constant would not be relevant. To sum up, since very fast signals are evaluated, several difficulties arise.

To check this hypothesis it is necessary to move forward with the simulation. A capacitor of 10 pF is evaluated for the same circuit. The time necessary to fully charge it can be previously calculated.

$$5 \cdot \tau = 5 \cdot R \cdot C = 5 \cdot 6 \cdot 10^{-12} = 0.03\text{ ns}$$

In this case, the time to fully charge the capacitor is smaller than the rise time, therefore, the capacitor could be fully charged.

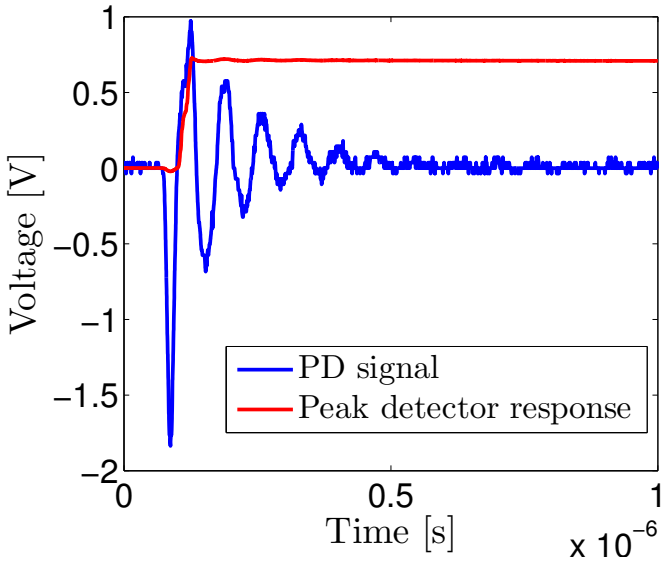


Figure 33: Peak detector for 100 pF capacitance

As foreseen, the peak detector works properly since the charging time is smaller than the rise time of the signal as Figure 33 points out.

The voltage is set to a value near the peak value because the diode is a non ideal component and a voltage drop is produced across the diode. In addition, as it was exposed, the diode blocks the current to flow back, setting the value of the output.

Another important fact to analyse is the signal shape. As exposed in Chapter 2 the circuit that allows to detect partial discharge can be represented as a RLC circuit, the resistance is present in the cables and several capacitors and a coil are included in the detection circuit (see Figure 9).

Accordingly, taking into account [31], the response of the partial discharge could be compared with a damped sinusoid, this is a sinusoidal function whose amplitude tends to 0 when the times goes on. The result is exposed in Figure 34.

The blue line represents the partial discharge signal obtained following the Standard method, the red line is a damped sine wave that can be compared with the partial discharge signal. The approximation is pretty good since the red line is very similar to the blue one. A typical damped sinusoid has the following structure.

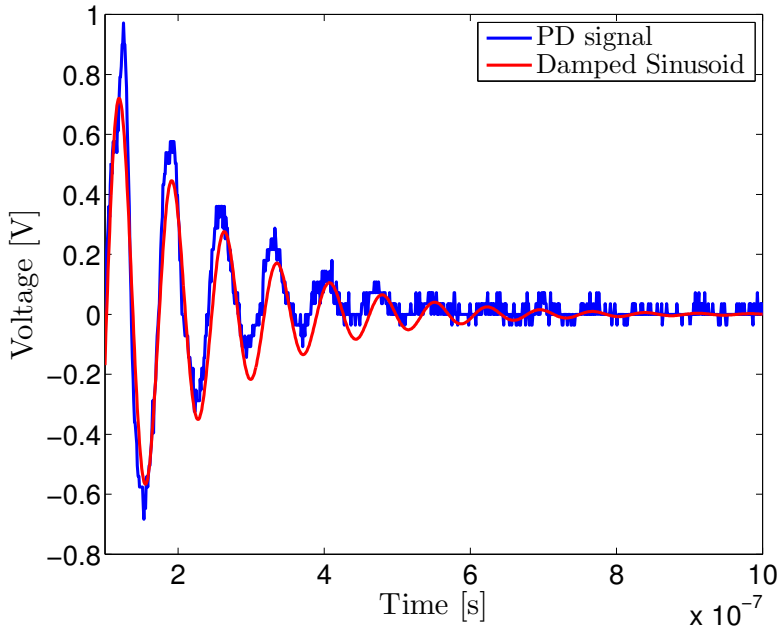


Figure 34: Comparisson with dumped sinusoid

The importance of this comparison resides in that a better understanding of the signal may help to simulate the feasibility of charging the capacitor. Besides, if it is not possible to access the laboratory in order to collect real signals, a signal could be created following this explanation.

$$y(t) = A \cdot e^{-b \cdot t} \cdot cos(C \cdot t + D) \tag{29}$$

where A, B, C and D are constant whose meaning and value is listed in Table 5.

| **Name** | **Meaning** | **Value** |
|---|---|---|
| A | Amplitude of the envelope | 1.6 V |
| B | Decay constant | $6.66 \cdot 10^{-6}\ s^{-1}$ |
| C | Pulsation | $8.72 \cdot 10^{-7}\ s^{-1}$ |
| D | Phase angle at t=0 | $-\pi/3$ |

Table 5: Damped sinusoid parameters

# Chapter 6

# Laboratory results

After the simulation through Pspice it is mandatory to check the real response of the circuit. Several measurements were taken varying the level of voltage. The circuit implementation is the same that for the simulation in Pspice, a breadboard was used to join the components.

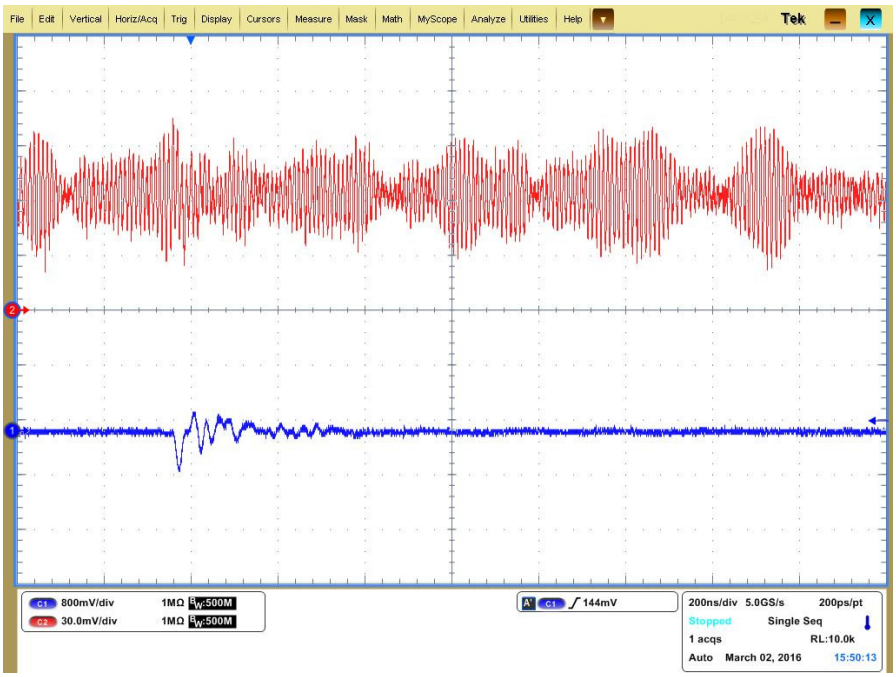


Figure 35: Partial discharge activity for 3000 V

In Figure 35, it is shown an image from the oscilloscope. In this case the polarity of the circuit has been inverted because partial discharge activity was more

pronounced in the negative half.

Channel 1, in blue color, is the partial discharge signal with an scale of 800 mV/div, so the peak of the PD signal is approximately 800 mV and in the channel 2, in red color, of the oscilloscope can be appreciated the response of the peak detector with an scale of 30 mV/div. The time scale is set to 200 ns/div.

The signal is difficult to analyse since electromagnetic noise is present, for this reason, for the next measurements, an average of the signal is enabled in the oscilloscope to observe clearly the output of the circuit.

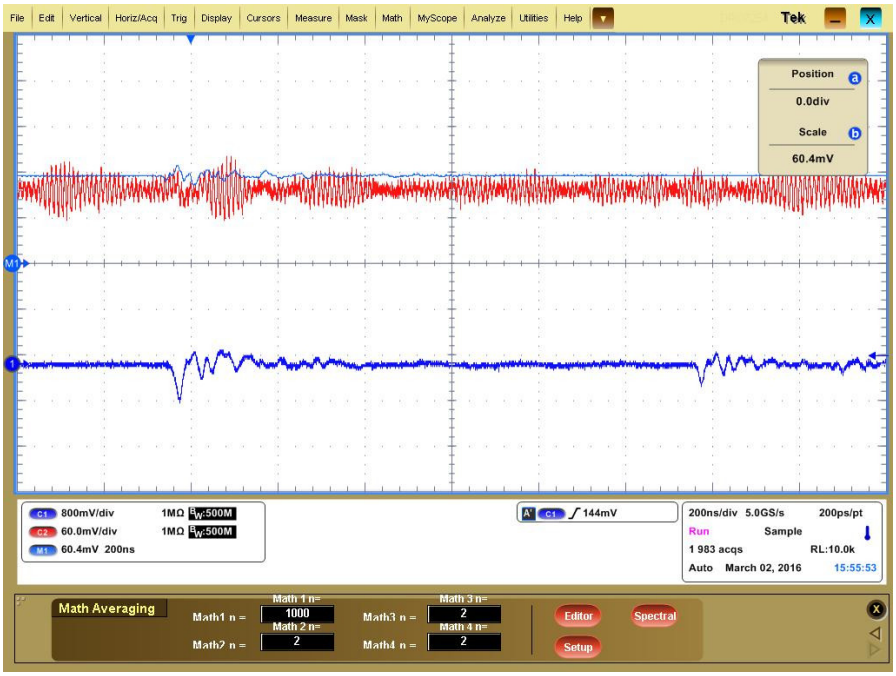


Figure 36: Partial discharge activity for 3600 V

Since the voltage applied is risen, PDs are expected to increase their activity so the scale of the channel 2 of the oscilloscope is modified up to 60 mV/div. In Figure 36, it is noticeable the light blue signal that represents the average of the output signal. The purpose of this signal is to visualize the average value of the signal so that there are no mistakes in the measuring.

The average value of the output is close to 120 mV, and it remains constant because the diode of the peak detector blocks the current to flow back to the source.

As the voltage is increased, PD activity is also higher. For Figure 37 the voltage across the capacitor, that is the output of the circuit, is around 180 mV.

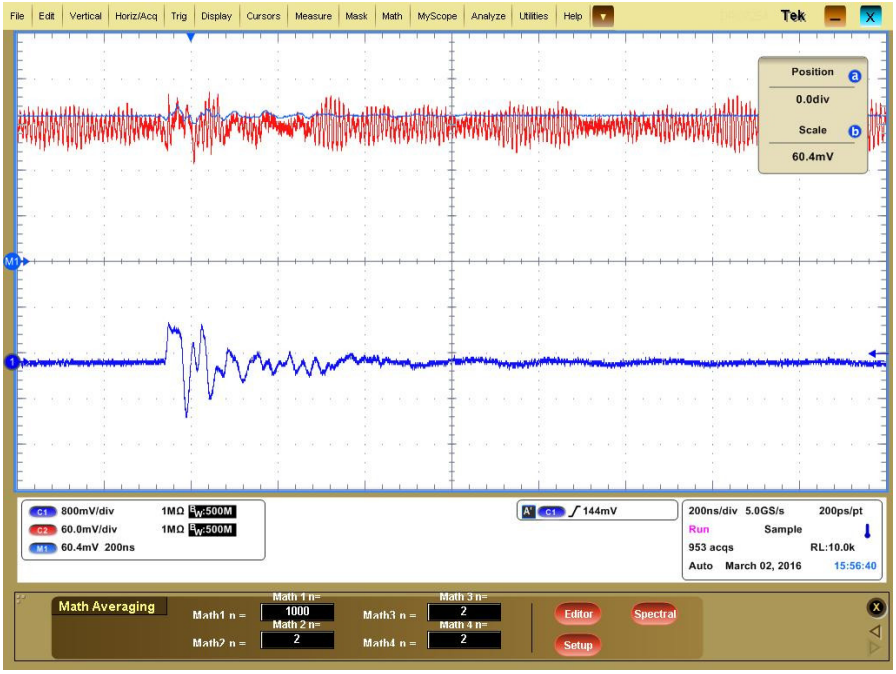


Figure 37: Partial discharge activity for 4000 V

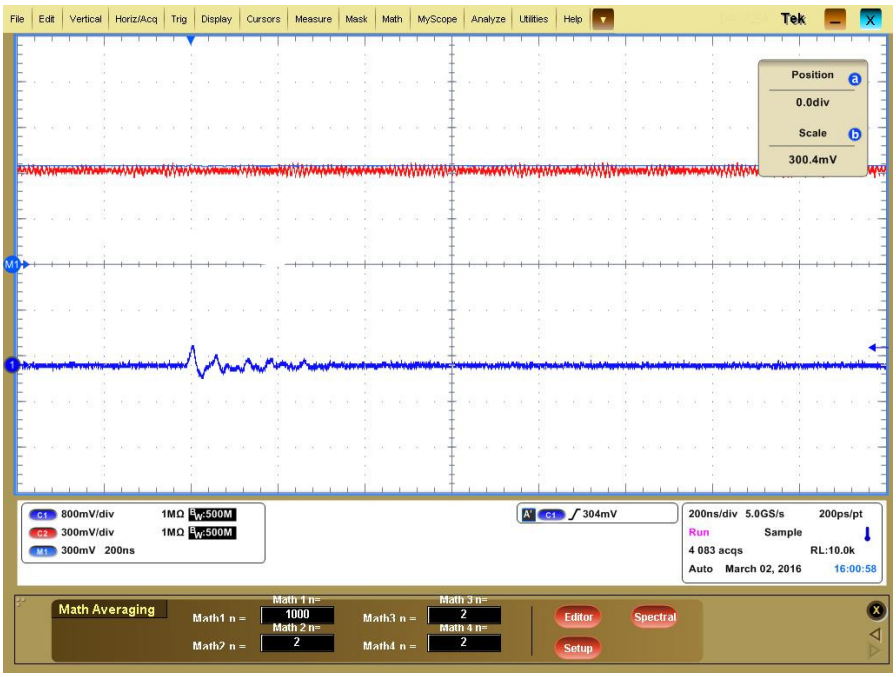


Figure 38: Partial discharge activity for 6000 V

The last of the simulations is carried out with a maximum voltage of 6000 V. It is recommended not to rise the voltage over this value in order to protect the oscilloscope, because it might be dangerous.

In Figure 38 the voltage rise is up to 700 mV, this fact makes sense because the higher the voltage source value, the higher the output of the circuit since it is proportional to the presence of PD signals.

In conclusion, energy has been harvested from PD pulses in a capacitor. When PDs activity is steady, if the voltage is raised, the presence of PD signals become more pronounced but after certain time, it becomes steady again. The result of the real test is pretty similar to the previous simulation since the voltage across the capacitor is near 0.7 V in both cases. The energy harvested was calculated approximately after the simulation (see (28)).

# Chapter 7

# Booster

Despite having accumulated energy in a capacitor, the available energy is really low. A booster can be joined to the circuit in order to increase the voltage across the capacitor.

A booster is a DC-DC converter that step up the input voltage when it is higher than a pass-through threshold, but taking into account that the power ($P = V \cdot I$) must be conserved, the output current has to be lower than the input current [32][33].

This electronic circuit is based on the configuration exposed in Figure 40. It is composed of a coil which accumulates energy in a magnetic field as long as the current flows. If the current changes, a voltage is induced in the conductor according to the Faraday's Law.

Two processes occur in the step up voltage:

- Charging phase. If the switch remains open for a long time the output voltage is equal to the input voltage, when the switch closes the diode prevents the capacitor from discharging (see On-State in Figure 39). The current through the inductor rises linearly at a rate proportional to the input voltage divided by the inductance and the load is powered by the capacitor.
- Discharging phase. When the switch is open again the current flows from the inductor through the diode in order to charge the output. See On-State in Figure 39. As the output voltage is increased, the current, $\frac{di}{dt}$ through the inductor is reversed.

To sum up, the output voltage is the input voltage with the contribution of the energy accumulated in the inductor.

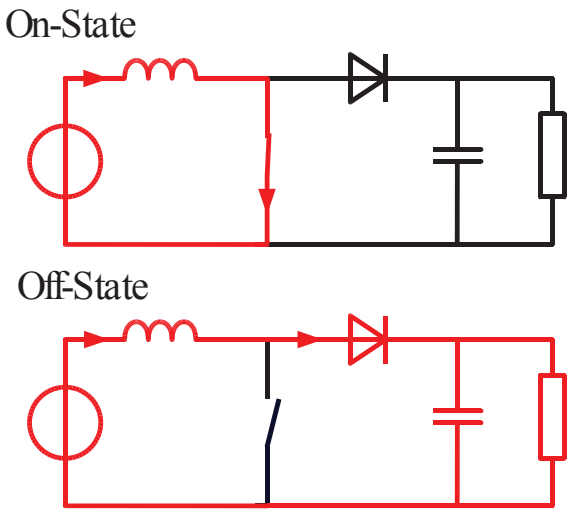


Figure 39: Simple boost converter states

The output voltage depends on the duty cycle of the switch, this concept is important to be introduced. It is the fraction of the switching period $T$ during which the switch is on, so the value of $D$ is constricted between 0 and 1.

According to [34], the output voltage can be expressed as:

$$V_o = V_{in} \cdot \frac{1}{1 - D} \tag{30}$$

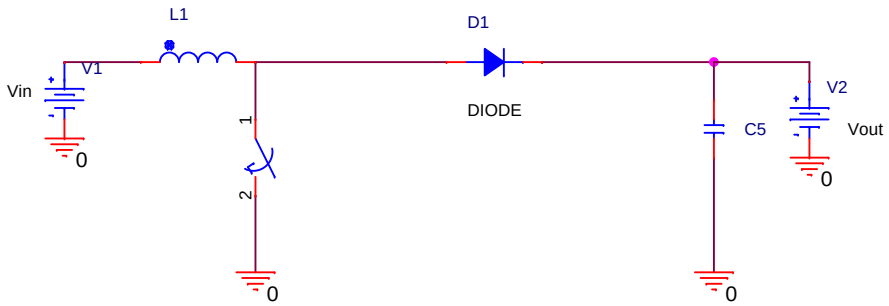


Figure 40: Simple boost converter circuit

To select the booster required it is important to notice that the maximum voltage across the capacitor is near 0.7 V and there is a voltage threshold that is needed to overcome in order to get an output voltage over the input.

In addition, it is fundamental to choose a boost with a great power efficiency. This is very important because the aim of this project is to accumulate energy then, power losses would affect this goal.

TPS610982 boost from Texas Instrument is the choice. The recommended voltage required in the input of the boost is 0.7 V, so this requirement is met. The output voltage is selectable up to 4.3 V and the efficiency is close to 90%.

Firstly, it is necessary to simulate the behaviour of the circuit in Pspice. The steps to design the coupling circuit for Pspice are given in the datasheet.

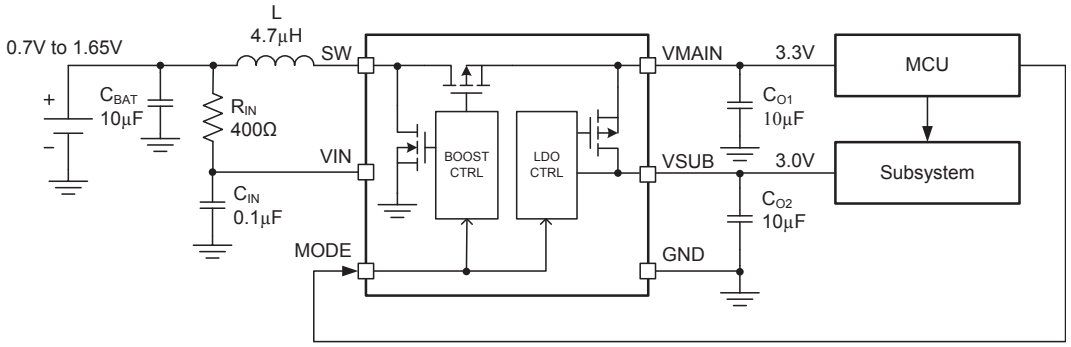


Figure 41: TPS2860 Booster from Texas instrument [35]

Every pin must be explained in order to understand this electronic device and its connection.

- SW pin is the connection for the inductor.
- VIN pin is the power supply input.
- MODE pin is a feature to control the mode. Active mode and low power mode are available. The first one activates two outputs (VMAIN and VSUB), the low power mode allows to activate only the VMAIN output. It is very important not to leave MODE pin floating.
- VMAIN pin is the output of the circuit with the boosted voltage.
- VSUB pin allows to supply another peripheral load if mode pin is active.
- GND pin is the ground of the circuit.

Further advices are given such as thermal considerations that are not going to be taken into account for this project.

So, following the recommended implementation by the manufacturer [35] shown in Figure 41 the consequent Pspice model can be achieved looking at Figure 42.

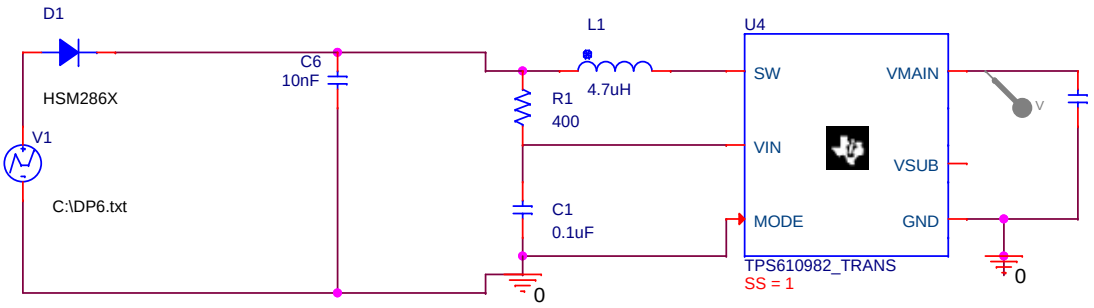


Figure 42: TPS2860 Booster Psice implementation

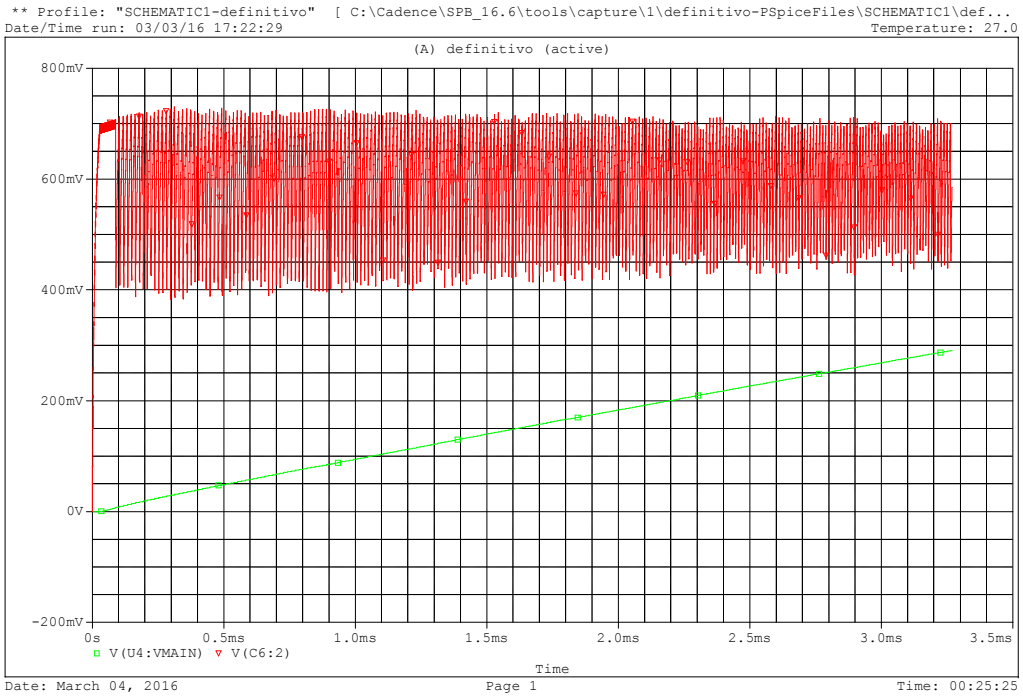


Figure 43: Simulation result

The simulation was not completed, a long time was required and an error during the simulation occurred. Several tries were carried out but the computer was not powerful enough to run the simulation. Even so, the result of the process is shown in Figure 43.

The signal represented in red colour is the voltage across the capacitor of 100 nF, it reaches a value of near 700 mV as it is checked in previous simulations but, in this case, it is an oscillating value between 400 and 700 mV. This can be caused by the presence of an extra load represented by the booster that absorbs energy from the capacitor.

On the other hand, the green signal is the boost output, i.e. VMAIN. In this case, the booster starts running because the input of the booster is over the threshold voltage but the time is not enough to notice a step up in the voltage since at 3 ms is stopped when the output voltage is close to 300 mV.

Since it is not a conclusive result the booster is tested at the laboratory, but the output voltage falls to 0.

As conclusion, this booster is not a good option to step up the voltage. One of the main reasons is that the minimum input voltage for the booster is near the voltage across the capacitor which means that more energy is demanded.

# Chapter 8

# Model extension

Power supply problems are present. The motive is that only positive half of the signal is being used since the diode only conducts in one sense. This inconvenient could be resolved by implementing a full wave rectifier [36].

Full wave rectifier consists of an electronic circuit composed of several diodes so that not only positive cycle half but negative one is rectified, it means more energy extractable to set the goal of harvesting energy closer.

It allows to convert AC or pulsing direct current from a low voltage to a higher voltage lever, a step up in the voltage is produced. The main advantage is that it produces a voltage rise using only diodes and capacitors, which means cheap devices. Indeed, several stages can be joined one each other to achieve a greater voltage.

The explanation of the circuit operation is exposed in Figure 44.

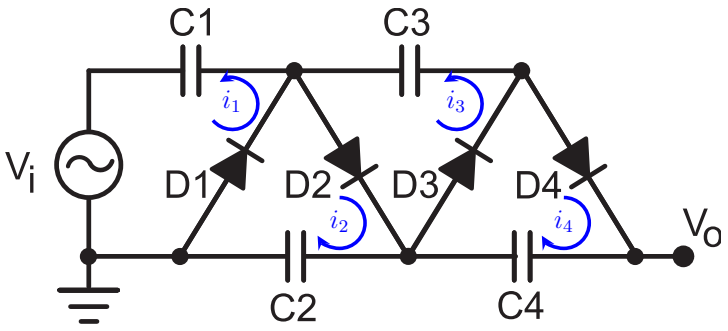


Figure 44: Cockcroft-Walton multiplier

Consider $V_i$ as an alternating current power supply with $V_p$ defined as the peak value of the input signal.

When the input voltage reaches the negative peak of $V_i$ signal, the current charges $C1$ capacitor through $D1$ diode to a value of $V_p$ with $i_1$ current. However, when the signal is reversed and the positive peak is reached, the current charges $C1$ up to $2 \cdot V_p$ and since $D1$ is reverse biased the current $i_2$ flows through $D2$ branch in order to produce a voltage across $C2$ of $2 \cdot V_p$.

In the next cycle, when the voltage is reversed again, $C3$ is charged to $2 \cdot V_p$ through $D3$ with $i_3$. At last, $C4$ is charged up to $2 \cdot V_p$ with $i_4$ flowing through $D4$ when the positive peak is reached.

Extrapolating on this idea, the output voltage is:

$$V_o = 2 \cdot n \cdot V_p \tag{31}$$

where $n$ is the number of stages. It is determined by the number of capacitors between ground and the output signal which in this case are capacitors $C2$ and $C4$.

It is important to say that in this explanation the forward voltage of every diode is not considered but it is an important fact that must be taken into consideration because for the real output voltage calculation, four voltage drops in the diodes are produced. Therefore, a lower voltage in the output is expected.

For this project purpose, a two stages multiplier is going to be implemented, the difference regarding Figure 44 is that a higher capacitance capacitor is added at the output voltage in order to storage energy, diodes from $D1$ to $D4$ are set to 1 pF and the output capacitor is set to 100 nF [37].

The response of $C1$ - $C4$ diodes is very fast because of its time constant equation (19) while the output capacitor response is slower since the capacitance is pretty smaller but the discharging process will also occur in a slower manner.

## 8.1. Pspice simulation

The next step is to analyse the behaviour of the circuit by implementing this model in Pspice, the diodes necessary to run the simulation are HSMS286x Schottky diodes from Avago Technology created in subsection 5.3 (See Figure 45).

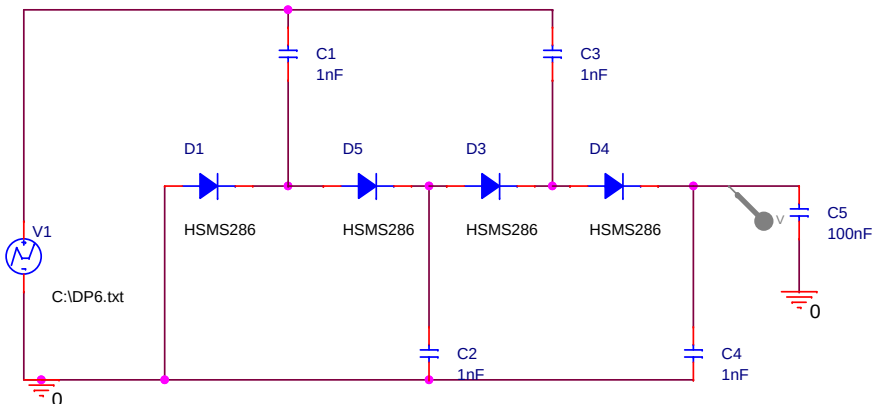


Figure 45: Cockcroft-Walton rectifier Pspice model

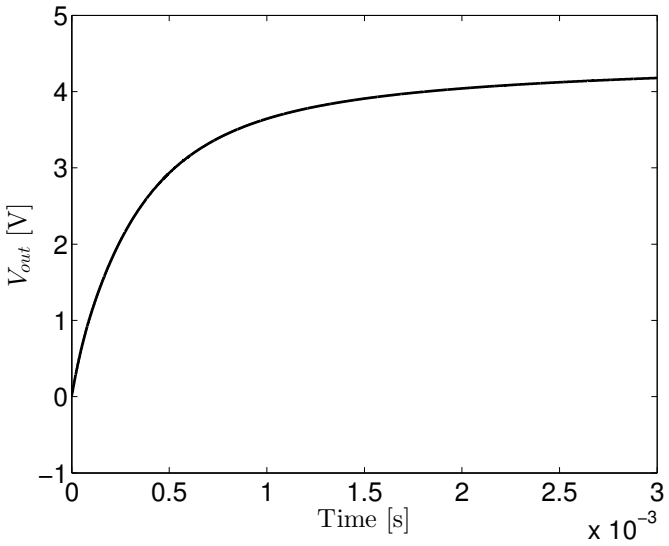


Figure 46: Cockcroft-Walton rectifier Pspice response

In Figure 46 it is exposed the output voltage of the two-stages Cockcroft-Walton rectifier. As expected the voltage across the $C5$ capacitor is much higher than the Figure 31 in spite of having set a shorter time for the simulation. The output voltage is around 4 V while using a simple rectifier this voltage is approximately 0.7 V, i.e. for the same input signal has been multiplied by more than five the voltage across the capacitor.

Regarding the investment, it is negligible since the price of diodes and capacitors is really low, so an improving has been carried out paying attention to economic

issues.

# Chapter 9

# PCB implementation

## 9.1. Definition

A simulation of a Cockcroft-Walton rectifier with Pspice was carried out and since the results were very satisfactory, a real model to check the real behaviour of this electronic circuit is required. Implementing this circuit in a breadboard is a tough task because the element size is really small and they must be soldered so the idea of creating a PCB arises.

A PCB is a connection of electronic components through electrical routes. They are etched from copper sheets laminated onto a non-conductive substrate. Depending on the component, it may be embedded or soldered. Besides, the PCB can be single sided or double sided, it is one or two copper layers and different layers are joined through a via.

## 9.2. Design

Modern PCB are implemented with layout software, following several steps. They can be summed up as follows:

- An initial schematic design is necessary through a Software.
- The card dimension must be adjusted depending on the component size.
- The components are placed taking into consideration the subsequent routing.

- The number of layers must be decided. It is strongly dependent on the circuitry complexity. In this step, it is important to define whether grounds plane are necessary or not, it would be the reference of the circuit.
- The clearance between different components is set in order to set a large enough gap to make easier the soldering of the elements.
- The components are routed following the schematic.
- Gerber files are processed by a CAD software to manufacture the PCB.

## 9.3. Eagle model

In this case, for implementing a PCB, *Eagle* software is the choice for its good performance and its strong electronic devices supply from different manufacturers. Previous steps are going to be followed to create a printed circuit board.

First of all, it is mandatory to develop a schematic, it is to conform the circuit exposed in Figure 45 but in Eagle software. Since every component involved in this circuit is included in Eagle libraries is not necessary to create a new model from an existing one as in Pspice case.

It is important to select the same diode because the package can vary depending on the model, in this case the recommended package by the manufacturer is SOT323.

Before creating the schematic, let check the package for HSMS286X diode provided by Eagle, so a comparison between the package dimensions supplied by the manufacturer and Eagle dimensions is done. It is a very important step because otherwise, it could cause problems in order to be soldered.

It is important to remark that this dimensions are exposed to a certain level of tolerance, as shown in Figure 47a.

In Figure 47b is shown SOT-323 Eagle package. One measuring is checked, the result of this is 2.09 mm and in Figure 47a the valid interval for $D$ measuring is between 1.80 - 2.25 mm so it is considered as a valid package.

In Figure 49 is implemented the schematic in order to create the PCB to carry out the simulation of a Cockcroft-Walton rectifier to increase the voltage across the capacitor and subsequently the energy extracted from PDs.

Since no simulation is going to be run, it is not necessary to import the voltage source but a SMA connector as the one shown in Figure 48 is required to take the signal from the PD origin to the PCB.

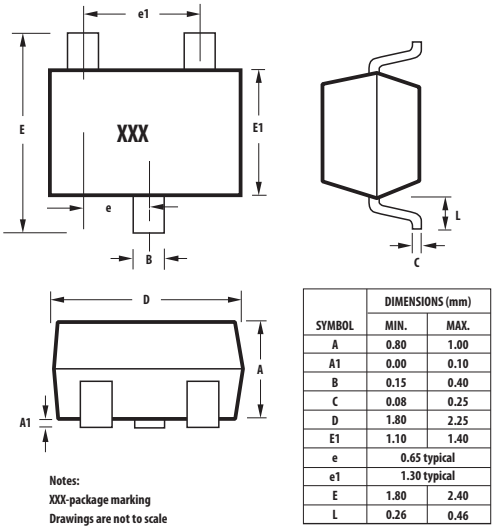


| SYMBOL | DIMENSIONS (mm) MIN. | MAX. |
|---|---|---|
| A | 0.80 | 1.00 |
| A1 | 0.00 | 0.10 |
| B | 0.15 | 0.40 |
| C | 0.08 | 0.25 |
| D | 1.80 | 2.25 |
| E1 | 1.10 | 1.40 |
| e | 0.65 typical | |
| e1 | 1.30 typical | |
| E | 1.80 | 2.40 |
| L | 0.26 | 0.46 |

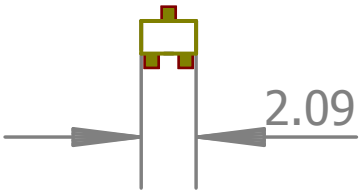


(a) Outline SOT-323 (b) SOT-323 Eagle package

Figure 47: Package comparisson [27]

Figure 48: SMA connector

The result of the schematic is shown in Figure 49 on the following page, the name of the elements is the same as Figure 46 in order to be consistent with the explanations. Regarding the SMA connector is represented as X2 in Figure 49.

In this case, it is not important to set the values of the components but the correct package to reach a good layout.

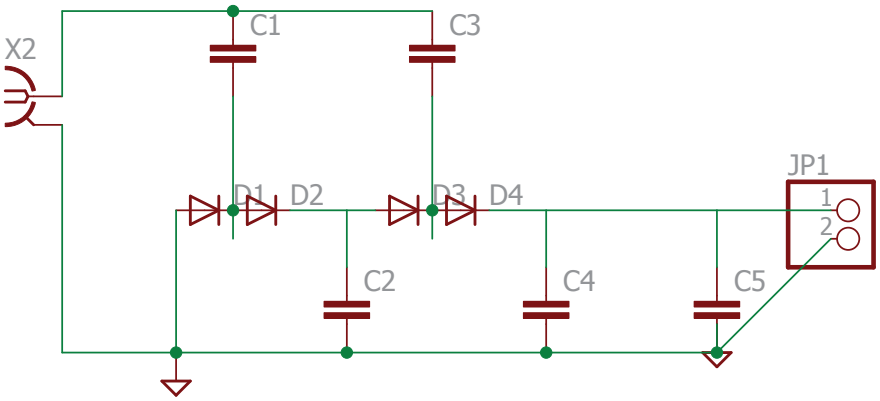


Figure 49: Cockcroft-Walton rectifier Eagle schematic

Once the schematic is completed the button "Switch to board" is pressed to access the menu of the board implementation in order to modify the features of the PCB.

A standard dimension is needed so a 3.5 × 5 mm board is the election, since the circuit is not very complex and the elements are small. The component are carefully placed considering the circuit topology and the layer is set to one. This is due to no ground plane is required and there is enough space in top layer to lay the whole circuit.

It is important to establish clearances between elements, element and route, routes, vias and pads regarding the soldering because if two points with different voltage are soldered a short-circuit is produced. The width of the route must be enough to facilitate the welding, in this case 1 mm width route is chosen.

Before routing the components a consideration has to be followed, right angles must be avoided considering that they prompt a higher copper concentration which generates a greater impedance. In addition, right angles produce an electrical field emission which may lead to an uncertain voltage transmission.

The next step is routing the components, Eagle software offers an "Autorouting" feature that routes every component automatically, in this case the circuit is routed manually to aim a better layout. The result of the PCB layout is in Figure 50.

Once the layout of the printed circuit board is completed, it is necessary to manufacture the board. This job is intended for Universidad Carlos III de Madrid workshop.

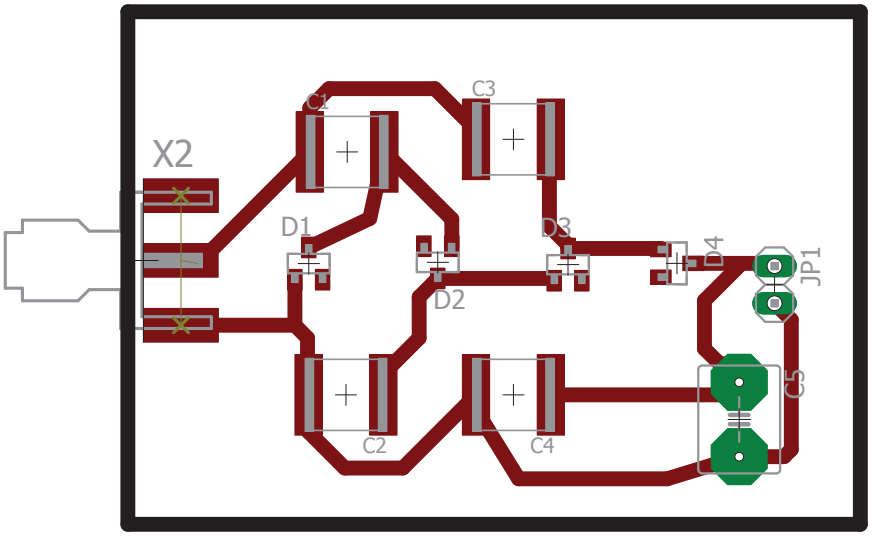


Figure 50: PCB layout

The information necessary to proceed is Gerber files. This format is an ASCII vector format for 2-D binary images. There are two mains types of Gerber format.

- Extended Gerber or RS-274X. This is the current Gerber format.
- Standard Gerber or RS-274-D. This format is obsolete. It is superseded by Extended Gerber.

For this project Extended Gerber is used. The files required are a top and a bottom layer file, another one containing the dimension of the board and a file which includes all the drills. This information is delivered to the workshop together with a real size figure because in case Gerber files are not recognised this image is enough to implement the PCB.

## 9.4. Real model

After delivering the precise information to the workshop, a PCB taking into consideration the layout conformed is received, the result is exposed in Figure 51.

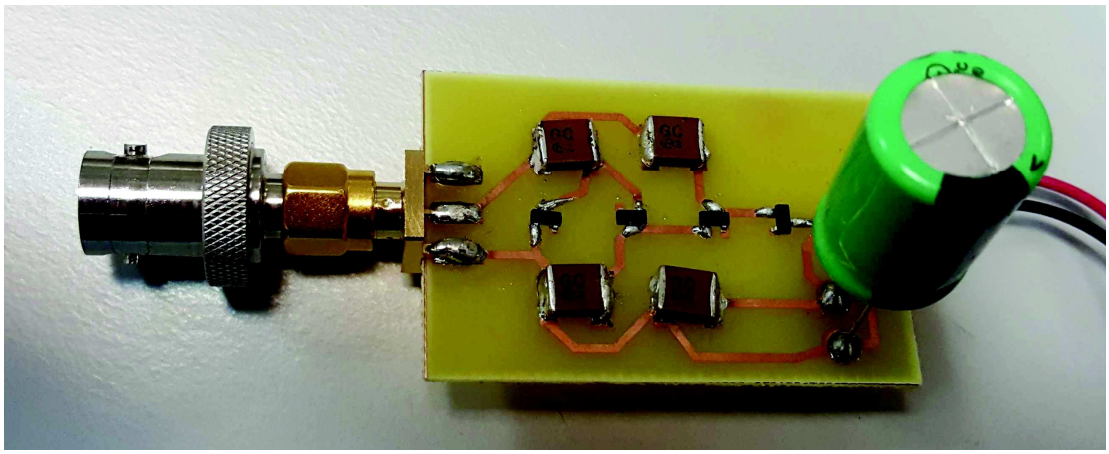

Figure 51: PCB result

The objective of creating a PCB is to check the response of the Cockcroft-Walton rectifier applied to PD signals. An analysis of the voltage across the capacitor is fundamental to estimate the energy stored because depending on the storage capacity a different purpose will aimed.

Providing the results are feasible, an external energy harvesting and boost module would be used in order to carry out an adequate power management.

Indirect circuit, as the one exposed in Figure 7 for PD detection following the conventional method, is again implemented at the laboratory. Cockcroft-Walton rectifier is intended to rectify and amplify the voltage from partial discharge signals.

The output voltage is near 1.5 V. Comparing with the simulation the voltage is fairly lower but with respect the peak detector case, which offers 0.7 V as maximum value, it is a great improving since the voltage is doubled. Regarding the energy stored in the capacitor, it can be calculated as follows.

$$E = \frac{1}{2} \cdot C \cdot V^2 = \frac{1}{2} \cdot 100 \cdot 10^{-9} \cdot 1.5^2 = 1.125 \cdot 10^{-7} \text{ J} \tag{32}$$

Accordingly, a ratio taking into account this energy accumulated from the voltage multiplier and the case with the peak detector is calculated.

$$Ratio = \frac{E_{multiplier}}{E_{peak}} = \frac{2.45 \cdot 10^{-8}}{1.125 \cdot 10^{-7}} = 4.59 \tag{33}$$

According to (33) near 5 times more of energy is stored thanks to the circuit

implemented. However, this energy is still a low figure so, in order to increase the energy storage capacity, a 1 mF capacitor was soldered in 100 nF place. This is due to the energy stored in a capacitor is affected linearly by the capacitance, i.e. if the same voltage is obtained in the capacitor, the energy stored would be $\frac{1 \cdot 10^{-3}}{100 \cdot 10^{-9}} = 10000$ times higher.

Another important factor that must be taken into consideration is the time constant. If the capacitance is raised, the time constant is linearly dependent on the capacitance so the time to fully charge the capacitor is also 10000 times higher. So in the PCB shown in Figure 51 the capacitor present is 1 mF capacitor not 100 nF capacitor.

Once the capacitor is changed, the voltage across the capacitor is 300 mV in one hour charging. The next step is to check the behaviour of an energy harvesting module.

## 9.5. Energy harvesting and Boost module

An improvement regarding the energy storage capacity has been carried out. In this case the energy scavenged is 5 times higher than the peak detector situation. Thus, an energy harvesting module can be included in the project in order to take the energy from the capacitor.

EH300 Energy Harvesting Module from *Advanced Linear Devices* is the election. This module is suitable for low power intermittent duty and long storage time applications [38].

The energy management of capturing, accumulating and storing small packets of energy requires high energy efficiency. The circuit of the energy harvesting module must stay in active mode in order to store energy whenever it becomes available and provide an output as required.

In this case, *Advanced Linear Devices* offers a booster and an energy harvesting module. This permits to step up the voltage across the capacitor even more in order to be stored later.

The requirement is an input DC voltage over 0 V with a current over 1 nA. From this value on, the booster steps up the voltage and after that the energy is accumulated thanks to the EH300 harvester module.

In Figure 52 it is exposed the necessary connection to join this device to the output of the voltage multiplier. The low voltage energy source comes from the output of the Cockcroft-Walton rectifier. Then, the link between EH4200 and EH300 modules is mandatory to provide a higher voltage. The energy is stored in EH300 module to carry out a purpose as for example powering an external load or charging a battery.

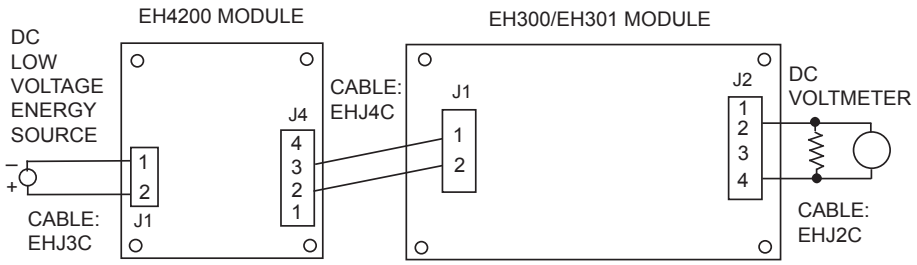


Figure 52: Module connection [38]

After connecting every component as explained, this circuitry is checked at the laboratory but the output voltage of the harvesting module is 0 and the capacitor is discharged. No explanation is found because the requirements are met and contacting the technical department of the manufacturer is required to find out about the occurring problem. After being replied, the response was not very clarifying which implied a petition for additional information but no further response was received.

# Chapter 10

# Final results

In spite of not having been able to use the energy harvester module, it is possible to store energy in a capacitor. The energy harvesting target is accomplished.

Harvester module uses a booster to step up the voltage but it is not necessary because of the Cockcroft-Walton rectifier utilization which steps up and rectifies the voltage.

Depending on the PD activity different energy levels will be stored in the capacitor. It is noticeable through the voltage across the capacitor, i.e. a relation between partial discharge occurrence and a voltage across the capacitor is done.

Hence, it is important to quantify the charging rate of the 1 mF capacitor. Several measurements are carried out at the laboratory to typify this variable.

There are several parameters involved in PDs activity. On the one hand, it depends on the voltage applied to the detection circuit. When voltage is applied, partial discharge phenomenon is present and it tends to become constant in approximately twenty minutes time, but if the voltage is raised again, partial discharge activity is increased.

On the other hand, partial discharges appearance is affected by the time, that is, at the beginning of applying voltage, PD activity is more intense but it tends to decrease when the times goes on. Another important factor to describe is the trigger, if a low trigger is set, more acquisitions appear but these signals can be electromagnetic noise.

Each five minutes the value of the acquisitions of partial discharges provided by the oscilloscope is noted down and after that, the value is reset. It is expected to obtain a higher value at the beginning of applying voltage because PD activity

tends to become steady. So the first measuring is in $t = 5$, the second one in $t = 10$...

| **Time [min]** | **Acqs** | **Trigger [V]** | **Voltage [V]** |
|---|---|---|---|
| 5 | 8250 | 2 | 2145 |
| 10 | 4870 | 2 | 2145 |
| 15 | 3200 | 2 | 2145 |
| 20 | 2260 | 2 | 2145 |
| 25 | 2230 | 2 | 2145 |

Table 6: PD acquisitions at 2145 V

According to Table 6, it is noticeable that partial discharge activity decreases with time but it must be taken into account that partial discharges activity depends mainly on the insulation state. In this case the trigger is set to 2 V. Thus, signals under this value are not visualised, so it would be logical that if the trigger is set to a lower value, the number of acquisitions present in the oscilloscope is higher.

The supply voltage is raised up to 3485 V and the time goes until the partial discharge activity is established. Two measuring are taken.

| **Time [min]** | **Acqs** | **Trigger [mV]** | **Voltage [V]** |
|---|---|---|---|
| 1 | 1573 | 320 | 3485 |
| 3 | 3100 | 320 | 3485 |

Table 7: PD acquisitions at 3485 V

It can be seen in Table 7 that the number of acquisitions have increased noticeably, this is for two reasons: the trigger has been lowered from 2 V to 320 mV prompting a higher number of signals detected by the oscilloscope and the voltage supply has been increased up to 3485 V. In this case, the number of acquisitions per minute is near 1500.

In conclusion, as expected PD activity depends on the voltage applied, and the time. As higher the voltage, greater the number of acquisitions. The trigger has only influence regarding the visualization since a low trigger allows more signals to be detected but it does not affect to the charging rate of the capacitor. At last, the PD activity declines with time.

To analyse the charging rate of the capacitor, a similar process is carried out. Varying the voltage supply three times, the value of the voltage across the capacitor

is noted down each minute. An average function is enabled in the oscilloscope to visualize the value of the voltage. Several examples are shown. In Figure 53 the voltage across the capacitor is near 22 mV, applying 2185 V. For the case of Figure 54 the voltage across the capacitor is 321 mV with a supply voltage of 3485 V.

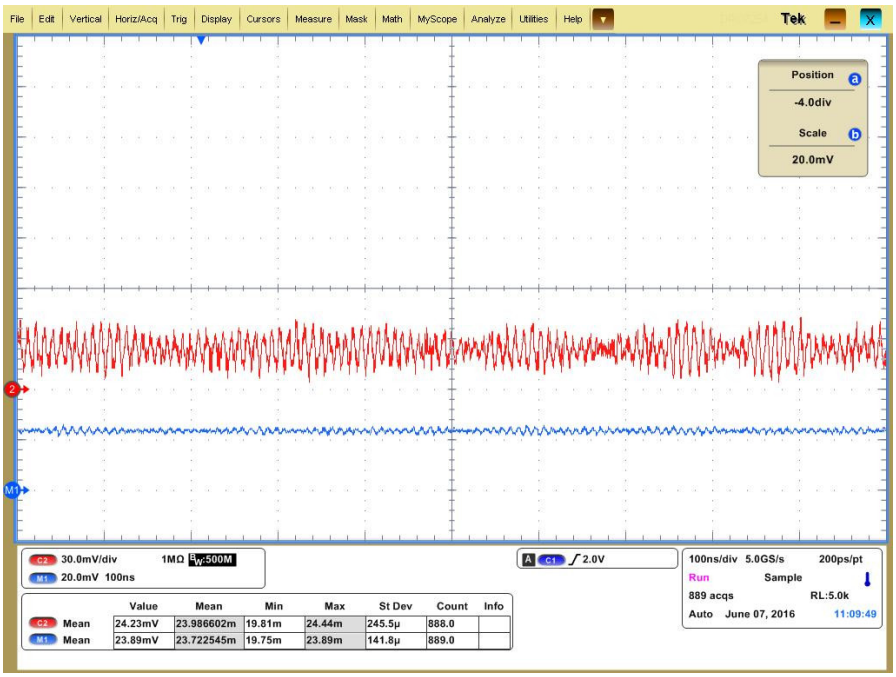


Figure 53: Capacitor charging rate 1

In Figure 55 it is shown the evolution of voltage across the capacitor, there are three differentiated stages because the supply voltage is modified three times.

At the beginning of every stage the slope is exponential but it tends to become steady at the end of the stage when the times passes.

It is noticeable that, depending on the voltage applied, the slope is different for every case. The slope is higher for 2985 and 3500 V cases since as it was explained, PD activity is more pronounced as higher the voltage.

For every situation, when PD activity becomes steady the rate of charging, i.e. the slope of the ending part in every stage, is near 1 mV/minute as exposed in Figure 55.

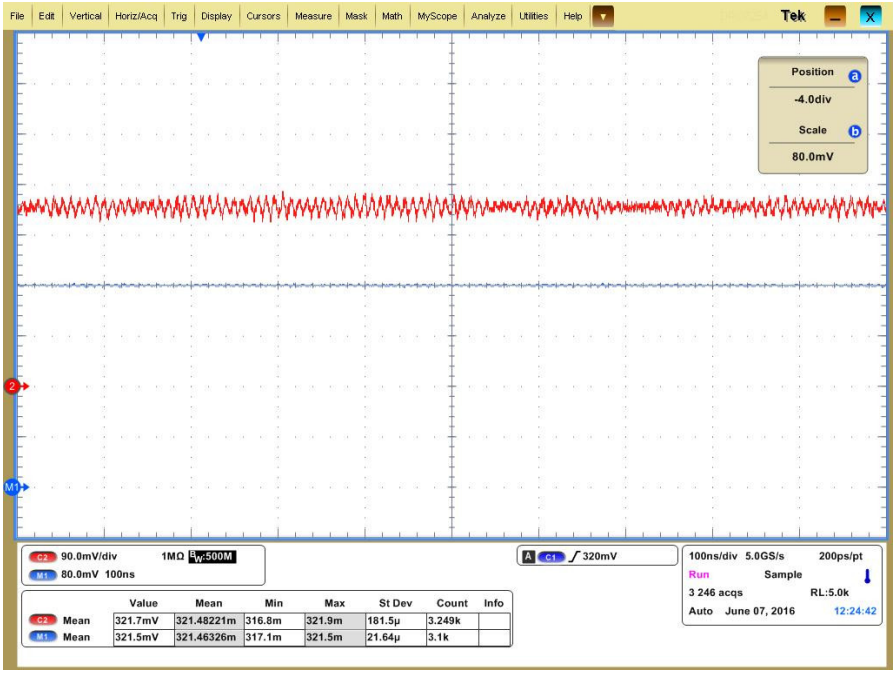


Figure 54: Capacitor charging rate 2

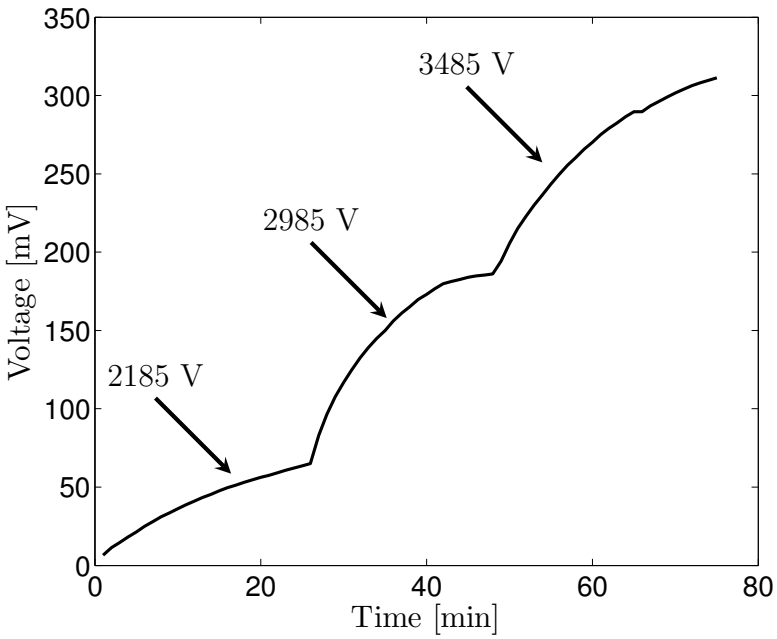


Figure 55: Voltage rise

# Chapter 11

# Conclusion and Future work

## 11.1. Conclusion

This thesis demonstrates how to harvest energy from partial discharge signals. A relation between partial discharges activity and a voltage in a capacitor is established. It is shown different configurations in order to store different energy levels in a capacitor.

This report can be structured in various stages. Firstly, partial discharge signals are detected following the conventional method exposed in the Standard. Once the signal is detected, Matlab allows to estimate the extractable energy is done. Thus, a first idea arises, it is calculated the time necessary to fully charge a 3.2 V and 0.7 mA·h battery, but this plan was rejected since it could not be tested at the laboratory due to its long time requirement, approximately 660 hours were needed to fully charge the battery in an ideal case.

After that, because of these signals are very particular with regard to its duration and shape, a deeper study to find a speed enough diode to rectify the signal is unavoidable. The choice was HSMS286x Schottky diode, so the peak detector circuit is composed of this diode to rectify the signal and a capacitor to accumulate energy.

Different simulation was run in Pspice to determine the best topology and the circuit was tested at the laboratory. As this project exposes the result is satisfactory, energy is harvested. Therefore, a booster module was tested with views to step up the voltage across the capacitor but it did not work. It may be due to the voltage across the capacitor was occasionally under the minimum input voltage required in the booster.

At last, since the energy accumulated in the capacitor is small, an extension of the model is presented. A voltage multiplier circuit is simulated in Pspice and, as expected, the energy storage capacity is signally increased, so to check the real model a PCB is designed and manufactured. The outcome of the real circuit provides five times more energy than the previous situation. Additionally, a harvester module was connected to the output of the multiplier but the energy stored in the module was zero. The project went forward without this module.

Since energy is harvested, it is important to quantify the charging rate of the capacitor that is the storage element. Several conclusions can be remarked. As higher the voltage applied to the PD detection circuit, higher is the initial rate of charge of the capacitor, but when the times goes on, regardless of the voltage, the charging rate tends to become constant near a value of 1 mV per minute. To typify this phenomenon, several measuring are exposed and explained during the report.

The maximum voltage across a 1 mF capacitor was 300 mV in one hour which implies a energy of 45 $\mu$J. This energy is not high enough to power a sensor as aimed at the beginning of the project. A later idea of turning a Led on arose, but a simulation run with Pspice shown in Figure 56 demonstrates that it could be turned on for less than a second because the led needs a current flowing over 5 mA to be turned on. This idea was also rejected because there is no point in turning a warning led for less than a second.

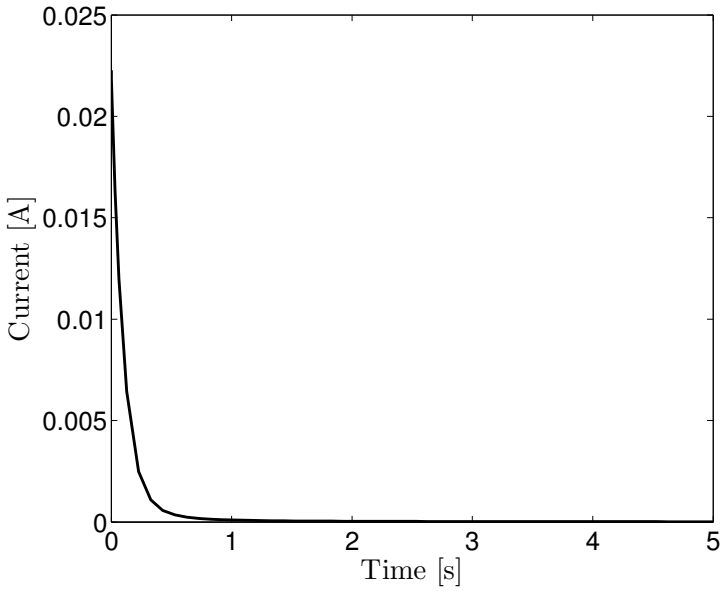


Figure 56: Led response

Summing up, the aim of the project, i.e. harvesting energy from inductive phenomena, is accomplished. In particular, the feasibility to extract energy from partial discharge signals is studied with a satisfactory result. A relation between energy stored in a capacitor and insulation status is established in this report. Further analysis can be carried out taking into consideration this report for future improving.

## 11.2. Future work

Regarding the good results exposed during the whole project a further step is thought. Energy has been stored in a capacitor by implementing an electronic circuit, but in order to show the voltage across the capacitor, that is, the partial discharges activity level, a deeper circuitry could be carried out.

An Arduino which is a microcontoller could be joined to the output of capacitor. A microcontroller is a self-contained system with peripherals, memory and a processor that can be used as an embedded system. They are present in PCs, mobiles phones and almost in every electronic device [39].

Arduino is a low cost microcontroller that allows to manage complex situations in a very easy way. It is also an open software suitable for electronic beginners. Arduino UNO board is based on ATmega328 microcontroller which contains 14 digital inputs and outputs but six of them can be used as analogical inputs. It also has an own programming language very easy to understand. Arduino UNO board is shown in Figure 57.

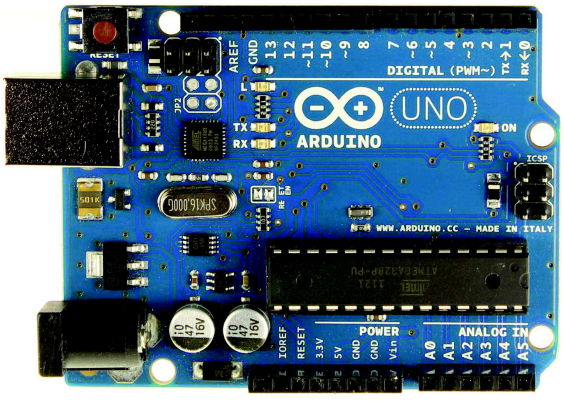


Figure 57: Arduino UNO Board

A possible improving of this project would be take the output voltage of the capacitor to an analogical input in order to be read. Once this value is stored, depending on the figure, a display in a LCD could be shown exposing the partial discharge activity and so avoid future failures of the electrical equipment.

Once the microcontroller is programmed, it would be able to detect a change in the charging rate of the capacitor, warning of a rise in PD activity. In addition, in order to minimize the power consumption and the capacitor discharging, a sleep mode can be used. By doing that, Arduino could read the voltage across the capacitor value and go to sleep mode until a new measurement programmed by the user is required.

# Chapter 12

# Project planification

Since this project contains a strong experimental load, scheduling a program before starting the project is a tough task because the evolution of this process depends strongly on the results obtained.

Nevertheless, a Gantt chart is exposed. There are three principal groups involved in the project realization:

- Documentation. It includes the steps necessary to understand the information related to energy harvesting and partial discharge concepts.
- Experimental measuring. In this group is involved, not only the time spent on the laboratory, but also the hours required to learn how to use simulation software such as Pspice or Eagle, implementing the Matlab code.
- Report redaction. The writing task explaining the whole project with its subsequent review.

It is noticeable that there are finish-to-start restrictions that point out that a task can not begin until its predecessor is finished, for example the information collected can not be understood before being found.

The milestone refers to the aimed target of extracting energy approximately accomplished in the second week of March.

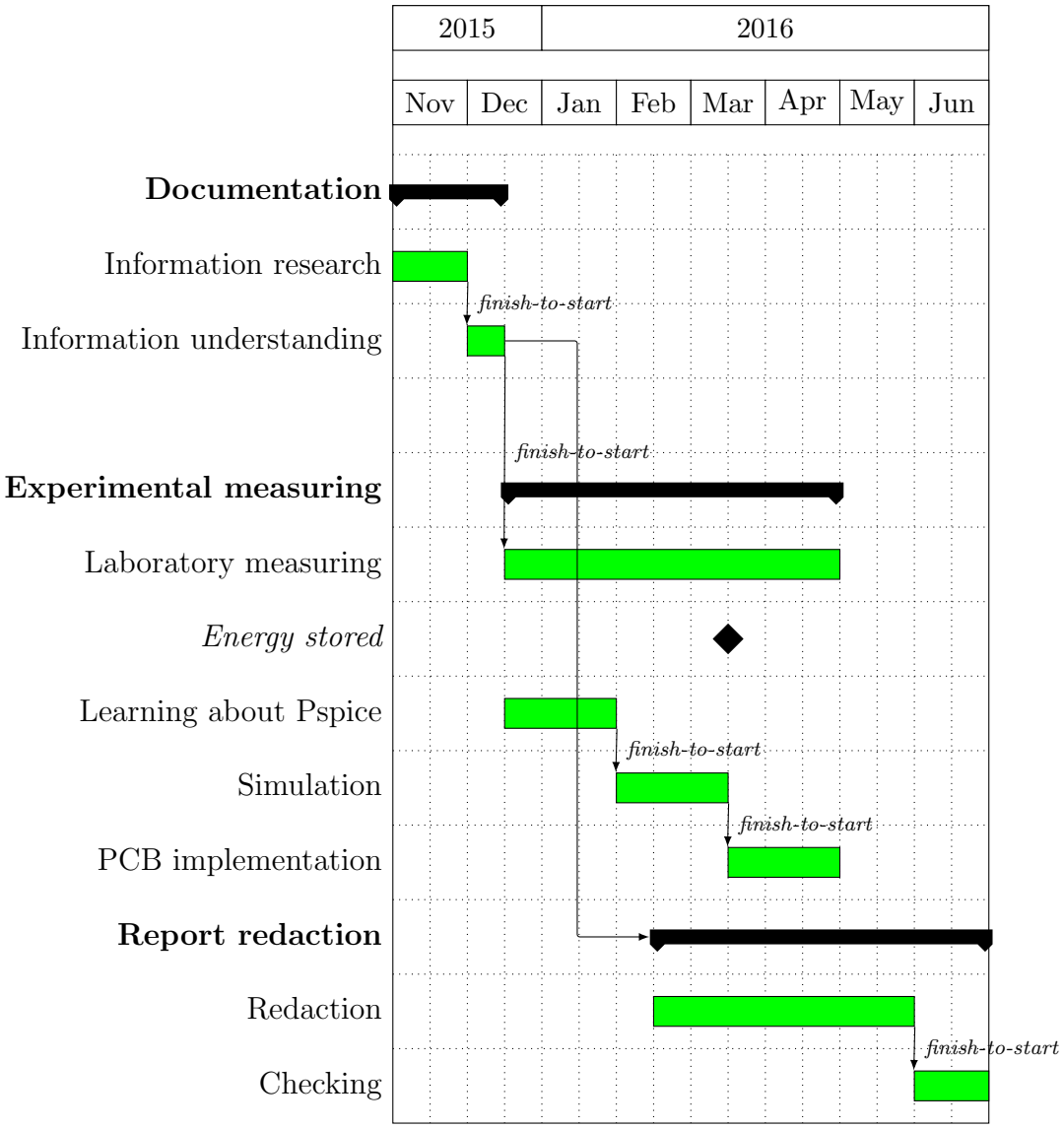
2015
2016
Nov
Dec
Jan
Feb
Mar
Apr
May
Jun
**Documentation**
Information research
Information understanding
*finish-to-start*
*finish-to-start*
**Experimental measuring**
Laboratory measuring
*Energy stored*
Learning about Pspice
*finish-to-start*
Simulation
*finish-to-start*
PCB implementation
**Report redaction**
Redaction
*finish-to-start*
Checking

# Chapter 13

# Budget

As in every project, the economical aspect is very relevant. So after the execution of every task involved, a detailed summary is essential. It is remarkable that this budget is only an approximation, which does not represent faithfully the reality.

It is important to say that diet and travel costs are not included in this project because this sort of expense has not been necessary. For the rest of the costs, an approximation of the depreciation periods is done in order to adapt the cost to the time usage.

| **Human Resources** | | | | |
|---|---|---|---|---|
| **Name** | **Category** | **Dedication (months)** | **Salary €** | **Cost €** |
| Molina Sanz, Javier | Junior Engineer | 8 | 2000 | 16000 |
| **Total cost: 16000€** | | | | |

Table 8: Human resources costs

| **Software** | | | | | |
|---|---|---|---|---|---|
| **Details** | **Quantity** | **Dedication (months)** | **Depreciation periods(months)** | **Unity cost €** | **Imputable cost €** |
| Matlab R2014 License | 1 | 6 | 24 | 2000 | 500 |
| Eagle License | 1 | 2 | 24 | 2000 | 166.33 |
| Orcad License | 1 | 6 | 24 | 2000 | 500 |
| **Subtotal cost: 1166.33€** | | | | | |

Table 9: Software costs

| **Hardware and electronic devices** | | | | | |
|---|---|---|---|---|---|
| **Details** | **Quantity** | **Dedication (months)** | **Depreciation periods (months)** | **Unity cost €** | **Imputable cost €** |
| Laptop | 1 | 8 | 60 | 800 | 106.6 |
| Osciloscope (Textronik DPO7254) | 1 | 6 | 60 | 21000 | 2100 |
| High voltage source | 1 | 6 | 60 | 6000 | 600 |
| HV Transformer | 1 | 6 | 60 | 9000 | 900 |
| Capacitor | 10 | 6 | 24 | 1 | 0.25 |
| HSMS286x diodes | 10 | 6 | 24 | 1 | 0.25 |
| TPS610982 Booster | 1 | 2 | 24 | 30 | 2.5 |
| EH4295+EH300 Module | 1 | 2 | 60 | 44 | 1.46 |
| SMA Connector | 1 | 2 | 24 | 10 | 0.83 |
| Coaxial cable | 1 | 6 | 24 | 5 | 1.25 |
| **Subtotal cost: 3713.14€** | | | | | |

Table 10: Hardware and electronic devices costs

| **Subcontracting** | | |
|---|---|---|
| **Detail** | **Provider** | **Cost €** |
| PCB implementation | UC3M | 50 |
| **Subtotal cost: 0** | | |

Table 11: Subcontracting costs

| **Budget area** | **Total cost €** |
|---|---|
| Human resources | 16000 |
| Hardware and electronic devices | 3713.14 |
| Software | 1666.33 |
| Subcontracting | 50 |
| **Subtotal costs: 21429.47€** | |

Table 12: Costs summary

| **Charge type** | **Percentig value (%)** | **Monetary value €** |
|---|---|---|
| Indirect costs | 15 | 3214.35 |
| VAT | 21 | 4500.09 |
| **Total costs: 29143.91€** | | |

Table 13: Final budget

# Bibliography


[1] J. R. Farmer, *A comparison of power harvesting techniques and related energy storage issues*. PhD thesis, Virginia Polytechnic Institute and State University, 2007.

[2] F. Blatt, P. Schroeder, C. Foiles, and D. Greig, "Thermoelectric power of materials," 1976.

[3] T. Douseki, Y. Yoshida, F. Utsunomiya, N. Itoh, and N. Hama, "A batteryless wireless system uses ambient heat with a reversible-power-source compatible cmos/soi dc-dc converter," in *Solid-State Circuits Conference, 2003. Digest of Technical Papers. ISSCC. 2003 IEEE International*, pp. 388–501 vol.1, Feb 2003.

[4] H. A. Sodano, G. E. Simmers, R. Dereux, and D. J. Inman, "Recharging batteries using energy harvested from thermal gradients," *Journal of Intelligent material systems and structures*, vol. 18, no. 1, pp. 3–10, 2007.

[5] V. Raghunathan, A. Kansal, J. Hsu, J. Friedman, and M. Srivastava, "Design considerations for solar energy harvesting wireless embedded systems," in *Proceedings of the 4th international symposium on Information processing in sensor networks*, p. 64, IEEE Press, 2005.

[6] A. Harb, "Energy harvesting: State-of-the-art," *Renewable Energy*, vol. 36, no. 10, pp. 2641 – 2654, 2011. Renewable Energy: Generation & Application http://www.sciencedirect.com/science/article/pii/S0960148110002703.

[7] E. Editors, "Tune in, charge up: Rf energy harvesting shows its potential," *Digi-Key Electronics*, May 2013. http://www.digikey.com/en/articles/techzone/2013/may/tune-in-charge-up-rf-energy-harvesting-shows-its-potential.

[8] F. Kocer and M. P. Flynn, "An rf-powered, wireless cmos temperature sensor," *IEEE Sensors Journal*, vol. 6, pp. 557–564, June 2006.

[9] H. R. Silva, J. A. Afonso, P. C. Morim, P. M. Oliveira, J. H. Correia, and L. A. Rocha, "Wireless hydrotherapy smart-suit network for posture monitoring," in *2007 IEEE International Symposium on Industrial Electronics*, pp. 2713–2717, June 2007.

[10] T. Taithongchai and E. Leelarasmee, "Adaptive electromagnetic energy harvesting circuit for wireless sensor application," in *Electrical Engineering/Electronics, Computer, Telecommunications and Information Technology, 2009. ECTI-CON 2009. 6th International Conference on*, vol. 01, pp. 278–281, IEEE, May 2009.

[11] T. T. Toh, S. W. Wright, M. E. Kiziroglou, J. Mueller, M. Sessinghaus, E. M. Yeatman, and P. D. Mitcheson, "Inductive energy harvesting from variable frequency and amplitude aircraft power lines," in *Journal of Physics: Conference Series*, vol. 557, p. 012095, IOP Publishing, 2014.

[12] L. Fish, "Power donut systems for overhead electric power line monitoring." http://www.usi-power.com/Products%20&%20Services/Donut/Power_Donut2_Qualifications.pdf, 10 2012.

[13] I. E. Commission *et al.*, *High-voltage Test Techniques: Partial Discharge Measurements*. International Electrotochnical Commission, 2000.

[14] H. Suzuki, K. Aihara, and T. Okamoto, "Complex behaviour of a simple partial-discharge model," *EPL (Europhysics Letters)*, vol. 66, no. 1, p. 28, 2004. http://stacks.iop.org/0295-5075/66/i=1/a=028.

[15] I. Standard, "High-voltage test techniques: partial discharge measurements," *IEC-60270*, 2000.

[16] F. Álvarez, F. Garnacho, J. Ortego, and M. Á. Sánchez-Urán, "Application of hfct and uhf sensors in on-line partial discharge measurements for insulation diagnosis of high voltage equipment,"

[17] G. Robles, J. M. Martínez-Tarifa, M. V. Rojas-Moreno, and J. Sanz-Feito, "Inductive sensor for measuring high frequency partial discharges within electrical insulation," *IEEE Transactions on Instrumentation and Measurement*, vol. 58, pp. 3907–3913, Nov 2009.

[18] M. M. Yaacob, M. A. Alsaedi, J. R. Rashed, A. M. Dakhil, and S. F. Atyah, "Review on partial discharge detection techniques related to high voltage power equipment using different sensors," *Photonic Sensors*, vol. 4, no. 4, pp. 325–337, 2014. http://dx.doi.org/10.1007/s13320-014-0146-7.

[19] L. E. Lundgaard, "Partial discharge. xiv. acoustic partial discharge detection-practical application," *Electrical Insulation Magazine, IEEE*, vol. 8, pp. 34–43, Sept 1992.

[20] A. C. Hernandez, "Manual pds100: Dispositivo portátil de inspección de descargas parciales mediante la medida de energía electromagnética en el espectro de rf.," Master's thesis, Universidad Carlos III de Madrid, July 2013.

[21] Mathuranathan, "Computation of power of a signal in matlab – simulation and verification." http://www.gaussianwaves.com/2013/12/computation-of-power-of-a-signal-in-matlab-simulation-and-verification/, December 2013.

[22] T. Ungan and L. M. Reindl, "Harvesting low ambient rf-sources for autonomous measurement systems," in *Instrumentation and Measurement Technology Conference Proceedings, 2008. IMTC 2008. IEEE*, pp. 62–65, IEEE, May 2008.

[23] W. Storr, "Rc charging circuit." http://www.electronics-tutorials.ws/rc/rc_1.html, August 2013.

[24] C. R. Nave, "Energy stored on a capacitor." http://hyperphysics.phy-astr.gsu.edu/hbase/electric/capeng.html.

[25] ScoolYouth, "Time constant and energy stored in capacitors." http://www.s-cool.co.uk/a-level/physics/capacitors/revise-it/time-constant-and-energy-stored-in-capacitors, 2016.

[26] I. Poole, "Understanding diode specifications & parameters." http://www.radio-electronics.com/info/data/semicond/diodes/specifications-parameters-ratings-characteristics.php.

[27] A. Technologies, *HSMS-285x Series Surface Mount Zero Bias Schottky Detector Diodes*. Avago Technologies, June 2012. http://www.avagotech.com/docs/AV02-1377EN.

[28] AllAboutCircuits, "Introduction to diodes and rectifiers." http://www.allaboutcircuits.com/textbook/semiconductors/chpt-3/introduction-to-diodes-and-rectifiers/.

[29] R. G. Harrison and X. Le Polozec, "Nonsquarelaw behavior of diode detectors analyzed by the ritz-galerkin method," *IEEE Transactions on Microwave Theory and Techniques*, vol. 42, pp. 840–846, May 1994.

[30] S. Wetenkamp, "Comparison of single diode vs. dual diode detectors for microwave power detection," in *Microwave Symposium Digest, 1983 IEEE MTT-S International*, pp. 361–363, IEEE, May 1983.

[31] S.-D. Yang, "Natural and step responses of rlc circuits." http://www.ee.nthu.edu.tw/~sdyang/Courses/Circuits/Ch08_Std.pdf. National Tsing Hua University.

[32] E. Coates, "Boost converters." http://www.learnabout-electronics.org/PSU/psu32.php, March 2016.

[33] "Dc-dc converter tutorial." https://www.maximintegrated.com/en/app-notes/index.mvp/id/2031, November 2001.

[34] C. Nelson, *LT1070 Design Manual*. Linear Technology, June 1986. http://cds.linear.com/docs/en/application-note/an19fc.pdf.

[35] SLVS873D, *TPS61098x Ultra-Low Quiescent Current Synchronous Boost with Integrated LDO/Load Switch*. Texas Instruments Incorporated, June 2015. http://www.ti.com/lit/ds/symlink/tps610987.pdf.

[36] AllAboutCircuits, "Voltage multipliers: Diodes and rectifiers." http://www.allaboutcircuits.com/textbook/semiconductors/chpt-3/voltage-multipliers/.

[37] T. Sogorb, J. V. Llario, J. Pelegri, R. Lajara, and J. Alberola, "Studying the feasibility of energy harvesting from broadcast rf station for wsn," in *Instrumentation and Measurement Technology Conference Proceedings, 2008. IMTC 2008. IEEE*, pp. 1360–1363, IEEE, May 2008.

[38] Advanced Linear Devices Incorporated, *EH300/301 EPAD® ENERGY HARVESTING MODULES*, 2015. http://www.aldinc.com/pdf/EH300.pdf.

[39] A. Chalkley, "The absolute beginner's guide to arduino." http://forefront.io/a/beginners-guide-to-arduino/, January 2013.